DEVELOPMENT OF A QUANTITATIVE MEASURE OF THE FUNCTIONALITY OF FRAME WALLS ENHANCED WITH PHASE CHANGE MATERIALS USING A DYNAMIC WALL SIMULATOR

by

Angela C. Evers

B.S. ME, Wichita State University, Wichita, Kansas, 1989

Submitted to the Department of Civil, Environmental, and Architectural Engineering and to the Faculty of the Graduate School of the University of Kansas in partial fulfillment of the requirements for the degree of Master of Science in Architectural Engineering

Committee:

____
Mario A. Medina, Ph.D., P.E., Chairperson

____
Thomas E. Glavinich, D.E., P.E.

____
Bedru Yimer, Ph.D.

Date Defended:________________________

The Thesis Committee for Angela C. Evers certifies
that this is the approved version of the following thesis:

DEVELOPMENT OF A QUANTITATIVE MEASURE OF THE FUNCTIONALITY OF FRAME WALLS ENHANCED WITH PHASE CHANGE MATERIALS USING A DYNAMIC WALL SIMULATOR

Committee:

____
Mario A. Medina, Ph.D., P.E., Chairperson

____
Thomas E. Glavinich, D.E., P.E.

____
Bedru Yimer, Ph.D.

Date Approved:________________________

ABSTRACT

The incorporation of phase change materials (PCMs) in building components for use as latent heat storage and for potential reduction of energy requirements is an on-going field of study. In this thesis, the development and testing of PCM-enhanced cellulose insulation for use in frame walls is presented. Three types of PCMs (paraffin-based, hydrated salt-based, and eutectic) were mixed with loose-fill cellulose insulation at various concentrations in a 1.19 m x 1.19 m (47 in. x 47 in.) frame wall cavity. The thermally-enhanced frame walls were heated and allowed to cool in a dynamic wall simulator that replicated the sun's exposure in a wall on a typical summer day. Heat fluxes, total heat flows, and surface and air temperatures were measured. Results from simulation testing showed that the paraffin-based PCM, RT27®, reduced the average peak heat flux by up to 9.2% and reduced the average total daily heat flow up to 1.2%. A powdered paraffin PCM, PX27®, reduced the average peak heat flux up to 9.3%, but did not decrease the total daily heat flow. Because of the hydroscopic nature of hydrated salts, the hydrated salt-based PCM and the eutectic salt/paraffin PCM did not provide any thermal storage benefit. Estimations of the equivalent thermal resistance for the paraffin-based PCM, RT27®, showed an increase of up to 60% when compared to the control wall.

ACKNOWLEDGEMENTS

I would like to enthusiastically acknowledge and express my thanks to all those who have supported me during my journey back into the field of engineering. To Dr. Mario A. Medina, thank you for your ever-present support and guidance. Your sponsorship has been invaluable and your dedication to the University, your students, your research, and to the fields of Architectural and Mechanical Engineering has been an inspiration. To my good friend Yuan Fang, thank you for all your help, patience, and companionship. It is my great honor to have had you as my lab partner for these past two years. To my co-researchers, Katie Molstad, Diane Basore, Silvia Reshmeen, Nikki Gibson, Oliver Meade, and Mashud Ahmed, thank you for your aid, ideas, and friendship. In the future, I hope to find as wonderful a team to work with as I have found in all of you.

To the faculty and staff of the School of Engineering, thank you for your assistance; and particularly to Dr. Tom Glavinich and Dr. Bedru Yimer, thank you for your support and participation on my committee. To Mr. Jim Weaver, Director of Laboratories, and Mr. Jay Barnard, Laboratory Technician, thank you for your immeasurable expertise and assistance. To Dr. Tom Mulinazzi and Mrs. Kathy Mulinazzi, thank you for your friendship, encouragement, and always-reliable advice.

To Central Fiber Corporation, particularly Mr. Dung Trieu, thank you for the testing, training, and expertise. To Dr. Scott White at JW Prairie Wind Power, thank you for your helpful collaboration. I would also like to gratefully acknowledge the contribution of the National Science Foundation for funding this research under Grant #0533362.

Finally, to my family and friends, thank you for always being there and believing in me; and most especially to my husband, Jim, and sons, Kirby and Nathan, thank you for being my foundation and my champions. Your encouragement and enthusiasm have meant the world to me, and without you, I would have never accomplished all that I have.

~Angie

TABLE OF CONTENTS

LIST OF FIGURES

LIST OF TABLES

CHAPTER I

INTRODUCTION

The purpose of this research was to evaluate the thermal performance of frame walls insulated with cellulose insulation mixtures enhanced with phase change materials (PCMs). The goal of this research was to develop a thermally enhanced, energy-efficient, building insulation with the potential to reduce peak heat transfer rates across walls, shift peak cooling loads, and reduce energy use in residential and small commercial buildings.

According to the U.S. Department of Energy [1], in 2005, residential and commercial buildings consumed 41.9 billion gigajoules (39.7 quadrillion Btu) of energy or 40% of the total primary energy consumed in the United States. In turn, the United States consumed 22.5% of the world's total energy. Of the total energy consumed in residential and commercial buildings, 23.3% was the result of space heating and 12.6% was the result of space cooling. The total energy demand in the building sector is expected to grow on average by 1.3% per year [1]. An effective approach to lower this energy consumption is with demand-side management, that is, by reducing the total energy buildings consume at the peak usage times. In most regions of the country, air-conditioning usage tops the list of peak energy consumption in buildings during the summer. One way to reduce this peak demand in buildings could be by using thermally enhanced building envelope components, such as incorporating phase change materials into traditional frame walls.

With the reduction of peak electric demand, there could be less of a need for electricity generation, and thus generating facilities and accompanying infrastructure. A decrease in electric generation could result in reduced use of fossil fuels and lowered emissions to the atmosphere. The use of PCMs in traditional building construction may result in energy savings and thus provide a direct financial savings to the consumer.

Cellulose insulation was selected as the means by which the PCMs were incorporated into the walls. Along with fiberglass (batt or loose-fill) and rock wool, cellulose is commonly used in the building industry to insulate walls and attics. Cellulose is made of paper fiber, mainly recycled newsprint and cardboard, and is formulated to satisfy fire rating, corrosiveness, odor, and fungi resistance standards imposed by the Consumer Products Safety Commission [2]. When applied, cellulose insulation fills the available airspace in a cavity, which may reduce air infiltration and increase the overall thermal efficiency of the frame wall. The thermal performance of cellulose insulation is comparable or better than other types of insulation. Loose-fill cellulose insulation has a higher R-value (0.256 m^2 K/W per cm, 3.7 ft^2 °F hr/Btu per inch) than that of batt fiberglass (0.220 m^2 K/W per cm, 3.2 ft^2 °F hr/Btu per inch) and a significantly higher R-value than loose-fill fiberglass (0.171 m^2 K/W per cm, 2.5 ft^2 °F hr/Btu per inch) or loose-fill rock wool (0.192 m^2 K/W per cm, 2.8 ft^2 °F hr/Btu per inch) [3]**.** Cellulose insulation is also non-toxic and irritant free.

There are two techniques used to install cellulose insulation: wet-spray and dry-blown. In the wet spray method, a small amount of water, mixed with a light adhesive, is added to the insulation as it is being blown onto to the interior of a frame wall. The cellulose adheres to the wall and any overspray is shaved off. The cellulose is then covered by the wallboard, creating the wall cavity. In the dry-blown or retrofit method, the cellulose is blown into existing wall cavities through holes drilled in the exterior siding. The result of these techniques is a densely packed cavity with little settling and minimal air gaps. In this research, the retrofit method was used to install the cellulose insulation in the test walls.

PCMs are specific chemicals that absorb heat from the surrounding environment while changing from solid to liquid. Conversely, as the environment cools, the PCM changes from liquid-to-solid and heat is released to the environment. The PCMs used in this experiment were engineered to fit a specific melting and freezing temperature range suitable for application in the exterior walls of buildings. When the PCM with a specific phase change temperature range is incorporated in frame walls, a part of the summer daytime heat, typically transferred to the indoor space, is stored in the PCM. This heat is later released back into the cooler environment, both indoor and outdoor, at night and early morning. Thus, with PCMs, space cooling load and total demand could be reduced.

PCMs are categorized by their thermal properties, specifically their melting temperatures and latent heat of fusion values, and are commonly divided into two groups: inorganic and organic. Inorganic PCMs used in thermal storage applications are typically salt-based products such as the hydrated salt PCMs detailed in Table 1. The hydrated salts are mixtures of anhydrous salt and water and are crystalline in their solid state. Beneficial to thermal storage applications, hydrated salt PCMs have a high latent heat value and a wide range of freezing temperatures. They are nonflammable, nontoxic, readily available, and inexpensive. Disadvantages of the use of hydrated salt PCMs are their corrosiveness, uneven melting (and thus, settling), and their susceptibility to supercooling. In supercooling, the hydrated salts, when heated in closed containers and then cooled, may not re-solidify until cooled to temperatures well below their melting point. If the PCM does not re-solidify, the absorption and release of latent heat (i.e., thermal storage) will not occur at the expected temperatures. Hydrated salts are also hygroscopic or tend to absorb moisture when exposed to air.

Table 1. Properties of Common Inorganic PCMs (adapted from [4])

PCM	Melting Point ºC (ºF)	Latent Heat of Fusion J/g (Btu/lbm)
$KF \cdot 4H_2O$ Potassium fluoride tetrahydrate	18.5 (65.3)	231 (99.3)
$CaCl_2 \cdot 6H_2O$ Calcium chloride hexahydrate	29.7 (85.5)	171 (73.5)
$Na_2SO_4 \cdot 10H_2O$ Sodium sulphate decahydrate	32.4 (90.3)	254 (109.2)
$Na_2HPO_4 \cdot 12H_2O$ Sodium orthophosphate dodecahydrate	35 (95)	281 (120.8)
$Zn(NO_3)_2 \cdot 6H_2O$ Zinc nitrate hexahydrate	36.4 (97.5)	147 (63.2)

Organic PCMs include various paraffins, fatty acids, alcohols, and esters. These have several beneficial properties for thermal storage. They have a high latent heat storage capacity, melt congruently, have no supercooling issues, and are nontoxic and noncorrosive. The properties of various organic PCMs are shown in Table 2**.** Paraffin PCMs have been popular in building applications in recent years and are formulated for thermal storage applications over a wide range of temperatures. The major disadvantage of organic PCMs is that they are flammable. Organic PCMs are also more expensive than hydrated salts.

A third category of PCMs may be identified as eutectics. Eutectic PCMs are a mixture of two or more PCM compounds in one of three combinations – inorganic/inorganic, organic/organic, and inorganic/organic. These mixtures are formulated to bring out the most desired properties of each of the compounds and typically have a high latent heat storage capacity, low flammability, and limited supercooling.

Table 2. Properties of Common Organic PCMs (adapted from [4])

PCM	Melting Point ºC (ºF)	Latent Heat of Fusion J/g (Btu/lbm)
$CH_3(CH_2)_{16}COO(CH_2)_3CH_3$ Butyl stearate	19 (66.2)	140 (60.2)
$CH_3(CH_2)_{11}OH$ 1-dodecanol	26 (78.8)	200 (86)
$CH_3(CH_2)_{12}OH$ 1-tetradeconol	38 (100.4)	205 (88.1)
$CH_3(CH_2)nCH_3$ or C_nH_{2n} n-Octadecane (paraffin)	20-60 (68-140)	~200 (~86)
45% $CH_3(CH_2)_8COOH$ 55% $CH_3(CH_2)_{10}COOH$ 45/55 capric-lauric acid	21 (69.8)	143 (61.5)
$CH_3(CH_2)_{12}COOC_3H_7$ Propyl palmitate	19 (66.2)	186 (80)

PCMs provide thermal storage for many applications including telecommunications, food service, transportation, clothing, hot and cold storage, space travel, waste heat recovery, and passive solar technology. The use of PCMs in buildings has been in development for many years. Adding PCMs into the building envelope provides thermal storage within the structure of the building and can be an effective barrier to unwanted heat transmission into the conditioned space. PCMs have been typically incorporated into the building structure in the form of impregnated masonry (brick or concrete block) or gypsum board in walls, ceilings, and floors [5]. PCMs have been macro-encapsulated in containers and microencapsulated by polymers to facilitate this incorporation [5]. Many applications of PCMs in the building structure have been found to be impractical, but most have been found to be beneficial as a method of heat storage. In all, the use of PCMs as thermal storage in buildings has great potential for energy savings, and thus cost savings.

CHAPTER II

LITERATURE REVIEW

The use of PCMs as thermal storage in buildings was studied as early as the 1970s. In 1974, Telkes [6] proposed the use of “heat of fusion” materials as a thermal storage medium in heating and cooling systems in buildings. The practice of incorporating phase change materials into the building envelope as a means of thermal storage has been investigated for several decades [4, 5, 6, 7, 8, 9, 10, 11, 12, 13, 14]. The goal of previous research was, as it still is, to find an effective, reliable, and practical means of incorporating PCMs into conventional building materials (e.g., the wall structure).

Hawes, et al. [4], and Feldman, et al. [7], investigated various methods of incorporating PCMs into gypsum wallboard and examined the performance of these wallboards. Organic PCMs (i.e., butyl stearate, dodecanol, propyl palmitate, and capric-lauric acid) were used in the experiments. A conventional wallboard was compared to a wallboard enhanced with PCM by direct incorporation (adding liquid PCMs into the gypsum at time of mixing) and by immersion (dipping of conventional wallboard in liquid PCM for several minutes). Hawes, et al., found that properties of the enhanced wallboards, such as strength, durability, stability, moisture absorption, and weight limits, remained comparable to those of conventional wallboards, and that the energy-storing capacity of the enhanced wallboard increased eleven-fold. Feldman, et al. [7], found through differential scanning calorimeter (DSC) tests that the thermal properties of PCMs incorporated in wallboards were unchanged even after several freeze-thaw cycles and that the storage capacity of PCM-enhanced wallboard was 12 times that of wallboard alone.

Scalat, et al. [8], conducted small-scale thermal storage tests by comparing the latent heat storage capacity of a room lined with PCM impregnated wallboard to a room with conventional untreated wallboard. They concluded that the PCM wallboards could be considered suitable for heat storage and may facilitate the shifting of the utility peak load as well as the increase of operating efficiency of space heating and cooling equipment.

Hawlader, et al. [9], investigated the microencapsulation of paraffin wax in polymeric films. Results from differential scanning calorimeter tests showed that the paraffin microcapsules had high heat storage and release capacities and were suitable for energy storage applications.

Zhang, et al. [10] tested the performance of macroencapsulated PCMs by developing a frame wall that incorporated paraffin PCM encapsulated in pipes. Two small-scale test houses were constructed to compare the thermally-enhanced walls in one house to conventional walls in the other house. Peak heat fluxes in each house were measured over several typical summer days. They concluded that the average peak heat fluxes in the PCM-enhanced frame walls were significantly reduced compared to the conventional frame walls, up to 20% lowered depending on the concentration of PCM (10% to 20% by weight of the wallboard).

Using the same small-scale test houses as Zhang, King [12] developed and tested the thermal performance of PCMs encapsulated in pipes in structural insulated panels (PCM-SIPs). King found, on average, a peak heat flux reduction of up to 60% for south facing walls enhanced with paraffin-based PCMs. Zhu [13] tested the thermal performance of King's PCM-SIPs using a dynamic wall simulator. Zhu concluded that the SIPs enhanced with paraffin-based PCMs achieved a lower peak heat flux of up to 34% when compared to that of the SIPs without PCMs.

Zhang, et al. [14, 15] developed and tested shape-stabilizing PCM consisting of 70% paraffin and 30% supporting material (polyethylene and styrene-butadiene-styrene block copolymer). Thermal performance tests of the PCM in both wallboard and floors in winter conditions found that the PCM wallboard and floor absorbed heat and narrowed the temperature swing in the conditioned space.

Kosny, et al., [16] developed a PCM-enhanced cellulose insulation using microencapsulated paraffin PCM in traditional frame walls. With a 5-hour heating cycle, they achieved up to a 40% reduction in the surface heat flow through the wall.

In summary, the research reviewed in this section showed that the application of PCMs into the building envelope can provide thermal energy storage and result in a reduction in peak energy requirements. However, these many past attempts to improve the energy efficiency of walls by the application of PCMs were met with mixed results [11]. Various PCMs were utilized for this purpose, which were mostly introduced by imbibing them into gypsum boards or by macroencapsulation. These systems demonstrated many advantages in peak load reductions, load shifting, and energy savings; however, three main problems limited their potential application: poor humidity transfer across the wall [10], the difficulty of installation in the case of macroencapsulated systems, and the difficulty of affixing paint or other wall finishes to the wallboard surface [17].

For these reasons, this research developed a system that not only offers the use of environmentally-friendly materials, but a systems in which the delivery of PCM to the building will be practical and will not compromise humidity transfer or the application of wallboard finishes.

Chapter III

Development of PCM-enhanced Cellulose Insulation

Six PCMs were selected to be mixed with the cellulose insulation for thermal performance testing: TH29-F127, TH29, TH24, RT27, SP25, and PX27. Most of these PCMs were mixed and tested in concentrations of 10% and 20% by weight of the wallboard. It should be noted that *all* concentrations of PCM mixed in the cellulose insulation were measured as a percentage of the weight of the wallboard. The paraffin-based PCMs, RT27 and PX27, were chosen to be mixed and tested at higher concentrations (30%, 40%). Four PCMs were applied to the cellulose in a liquid form. Two PCMs were powdered materials.

PCMs and their Properties

First, a coated hydrated salt PCM was developed by the Kansas Polymer Research Center at the Pittsburg State University in Pittsburg, Kansas. Essentially, this hydrated salt PCM was made by coating calcium chloride hexahydrate with polyurethane polymers that in other industrial applications had been successfully used to coat fertilizers and soybeans. High strength, insolubility to solvents, and low permeability to water were the desired characteristics of this polymer coating. Combined with the solid hydrated salt, the resulting material was a coated hydrated salt PCM that would be non-corrosive while maintaining good thermal stability. This coated hydrated salt PCM was named TH29-F127 (Figure 1) and was made with the commercially available hydrated salt PCM called TH29, made by TEAP Energy [18]. In its container at room temperature, the TH29-F127 had the appearance of white powder.

Figure 1. Coated Hydrated Salt TH29-F127 at Room Temperature

TH29-F127 was still being developed and final physical properties of the material had not yet been determined. A description and properties of TH29 are detailed below.

The un-encapsulated hydrated salt-based PCMs, TH29 and TH24 (Figures 2 and 3, respectively), manufactured by TEAP Energy, were chosen because of their high latent heat storage capacities, their non-flammability and non-toxicity, and because they melted at the desired temperature for use in walls. TH29 and TH24 were inorganic PCMs composed primarily of calcium chloride hexahydrate ($CaCl_2{\cdot}6H_2O$) with unknown (proprietary) additives. In their solid form, TH29 and TH24 had the appearance of white crystals. As liquids, TH29 and TH24 were clear and odorless. In Figures 2 and 3, both the clear liquid and the white crystals were present in the samples of TH29 and TH24 (more so in TH29) because the room temperature was very close to the melting temperatures of the PCMs. The properties of the hydrated salts TH29 and TH24 are shown in Tables 3 and 4, respectively.

Figure 2. Hydrated Salt-based TH29 at Room Temperature

Figure 3. Hydrated Salt-based TH24 at Room Temperature

Table 3. Properties of TH29 Hydrated Salt PCM (adapted from [18, 19])

Property	Description	
Appearance	White deliquescent crystals (solid)	
Melting Point (approx.)	29 ℃	(84.2 ℉)
Congealing Point	26 ℃	(78.8 ℉)
Latent Heat of Fusion	175 kJ/kg	(75 Btu/lbm)
Density Solid at 15℃ (59℉)	1.49 g/cm3	(92.4 lb/ft3)
Volume Expansion	No expansion	
Specific Heat Capacity (solid/liquid)	1.4 / 2.3 kJ/kg·K	(0.34 / 0.55 Btu/lbm·℉)
Heat Conductivity	1.0 W/m·K	(0.6 Btu/hr·ft·℉)
Flash Point	Nonflammable	
Corrosion	Corrosive	

Table 4. Properties of TH24 Hydrated Salt PCM (adapted from [20])

Property	Description	
Appearance	White deliquescent crystals (solid)	
Melting Point (approx.)	24 ℃	(75.2 ℉)
Latent Heat of Fusion	175 kJ/kg	(75 Btu/lbm)
Volume Expansion	No expansion	
Specific Heat Capacity (solid/liquid)	2.0 kJ/kg·K	(0.49 Btu/lbm·℉)
Heat Conductivity	1.0 W/m·K	(0.6 Btu/hr·ft·℉)
Flash Point	Nonflammable	
Corrosion	Corrosive	

The paraffin-based RT27 (Figure 4), manufactured by Rubitherm Technologies GmbH, Germany, was chosen because it had a high thermal energy storage capacity, was non-corrosive and nontoxic, and melted at the appropriate temperature for use in walls. RT27 was an organic PCM based on a mixture of n-alkanes with the molecular formula C_nH_{2n+2}. This chemical is most commonly known as octadecane and has the appearance of white crystals in its solid form. As a liquid, RT27 was clear and odorless. In Figure 4, mainly white crystals were present in the sample because the room temperature was likely lower than the melting temperatures of the RT27. The properties of paraffin-based RT27 are shown in Table 5.

Figure 4. Paraffin RT27 at Room Temperature

Table 5. Properties of RT27 Paraffin PCM (adapted from [21])

Property	Description	
Appearance	White crystals (solid)	
Melting Point (approx.)	28 ℃	(82.4 ℉)
Congealing Point	26 ℃	(78.8 ℉)
Latent Heat of Fusion	179 kJ/kg	(77 Btu/lbm)
Density Solid at 15℃ (59℉)	0.87 g/cm3	(54.3 lb/ft3)
Volume Expansion	10%	
Specific Heat Capacity (solid/liquid)	1.8 / 2.4 kJ/kg·K	(0.43 / 0.57 Btu/lbm·℉)
Heat Conductivity	0.2 W/m·K	(0.12 Btu/hr·ft·℉)
Flash Point	164 ℃	(327.2 ℉)
Corrosion	Chemically inert with respect to most materials	

A eutectic paraffin / hydrated salt PCM, SP25 (Figure 5), manufactured by Rubitherm Technologies, was chosen because it had a high thermal energy storage capacity, was nontoxic, and melted at the appropriate temperature for use in walls. SP25 was a mixture of both inorganic and organic compounds, specifically a preparation of paraffin and calcium chloride. In its solid form, SP25 appeared like a thick white paste. As a liquid, it had a blue gel-like appearance. In Figure 5, both the solid and liquid forms of the SP25 were present in the sample because the room temperature was very close to the melting temperatures of the PCM. By blending the inorganic and organic PCMs, SP25 had a lower flammability than paraffin, but remained corrosive. The properties of the eutectic SP25 are shown in Table 6.

Figure 5. Eutectic (Hydrated Salt / Paraffin) SP25 at Room Temperature

Table 6. Properties of SP25 Eutectic (Hydrated Salt / Paraffin) PCM (adapted from [22])

Property	Description	
Appearance	Blue paste-like gel	
Melting Point (approx.)	26 ℃	(78.8 ℉)
Congealing Point	25 ℃	(77 ℉)
Latent Heat of Fusion	180 kJ/kg	(77 Btu/lbm)
Density Solid at -15℃ (5℉)	1.38 g/cm3	(85.6 lb/ft3)
Volume Expansion	No expansion	
Specific Heat Capacity	2.5 kJ/kg·K	(0.34 / 0.55 Btu/lbm·℉)
Heat Conductivity	0.6 W/m·K	(1.5 Btu/hr·ft·℉)
Flash Point	Nonflammable	
Corrosion	Corrosive	

The powdered paraffin PX27 (Figure 6), also manufactured by Rubitherm Technologies, was chosen because it had a high thermal energy storage capacity, was non-corrosive and nontoxic, and melted at the appropriate temperature for use in walls. PX27 was composed of paraffin PCM bound within a silica powder as a secondary support structure and had the appearance of white powder. At temperatures found in building applications, this compound remained in a powdered form even when the paraffin PCM underwent phase change from solid to liquid and back again. In other words, the paraffin PCM changed into a liquid within the silica material and there was no leaking of the liquid paraffin outside of the supporting structure. The properties of powdered paraffin PX27 are shown in Table 7.

Figure 6. Powdered Paraffin PX27 at Room Temperature

Table 7. Properties of PX27 Powdered PCM (adapted from [23])

Property	Description	
Appearance	White powder (particle size: 250 µm	
Melting Point (approx.)	28 ℃	(82.4 ℉)
Latent Heat of Fusion	112 kJ/kg	(48 Btu/lbm)
Bulk Density	0.64 g/cm3	(39.9 lb/ft3)
Volume Expansion	No expansion	
Specific Heat Capacity	1.6 kJ/kg·K	(0.38 Btu/lbm·℉)
Heat Conductivity	0.1 W/m·K	(0.06 Btu/hr·ft·℉)
Flash Point	164 ℃	(327.2 ℉)
Corrosion	Chemically inert with respect to most materials	

Incorporation of PCM into Cellulose Insulation and Walls

The cellulose used in this research was Xcell® Cellulose Insulation (Figure 7) made by Central Fiber Corporation, Wellsville, Kansas [24].

Figure 7. Sample of Xcell® Cellulose Insulation

To incorporate the PCM into the insulation, the liquid/solid PCMs (RT27, TH29, TH24, and SP25) were melted in containers using a warm water bath. The liquid PCMs were sprayed onto the cellulose insulation, which was then manually mixed to distribute the material evenly (Figure 8). The powdered PCMs (TH29-F127 and PX27) were sifted, sprinkled, and manually mixed into the cellulose insulation. The PCMs were mixed in various concentrations as a certain percentage of PCM by weight of the wallboard.

Figure 8. Manually Mixing of Liquid/Solid PCMs

Each PCM cellulose mixture was installed in individual walls for testing. These walls were fabricated using standard wallboard construction techniques that consisted of 1.59 cm (5/8 in.) siding, 1.27 cm (½ in.) OSB sheathing, 5.08 cm x 10.16 cm (2 in. x 4 in.) framing, insulated wall cavity, and 1.27 cm (½ in.) gypsum wallboard with 40.64 cm (16 in.) stud framing. A wall cavity of approximately 81.3 cm x 111.8 cm (32 in. x 44 in.) or 0.91 m^2 (1408 in^2) resulted (Figure 9).

Figure 9. Wall Cavity Filled with Cellulose Insulation

The PCM cellulose insulation mixtures were blown into the wall cavities using the retrofit technique, which consists of dry blowing using an industry standard insulation blower. The blower used was an Intec Force/1 insulation blower (Figure 10). Specifications for this blower are given in Table 8. In the retrofit technique, the PCM cellulose mixture was loaded into the hopper and blown through a distribution hose inserted into holes drilled into the exterior of each wall. Insulation was first blown into holes drilled at the middle of the wall, and then blown into holes drilled at the top of the wall to ensure an even distribution of insulation material throughout the wall cavity. This procedure required specific training, which was provided by Central Fiber Corporation.

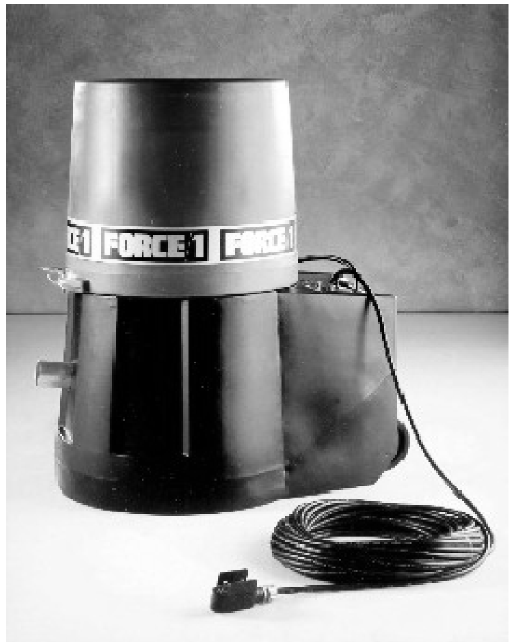

Figure 10. Force/1 Cellulose Insulation Blower [25]

Table 8. Specifications for Force/1 Cellulose Insulation Blower [25]

Product Specifications	
Height	104 cm (41 in.)
Width	82 cm (32-1/4 in.)
Weight	74.8 kg (165 lbs)
Hopper Capacity	11.3 kg (25 lbs)
Hose size	6.35 cm (2.5 in.)
Agitator Motor	0.6 kW (0.75 hp)
Blower	2.9 m^3/min (104 CFM)
Transmission	Direct drive
Electrical	115 Volt, 60 Hz, 20 Amp

CHAPTER IV

CONTROLLED LABORATORY TESTING USING A DYNAMIC WALL SIMULATOR

Test Series

The thermal performance of the PCM cellulose mixtures was tested along with the control insulation (unmodified) in a series of five tests. In the first series of tests, the thermal performance of two walls was tested: a wall enhanced with the coated hydrated salt TH29-F127 and a control wall. This contained the TH29-F127 in a concentration of 10%, by the weight of the wallboard, and is herein referred to as the TH29-F127 wall.

In the second series of tests, the thermal performances of four walls were tested: two paraffin walls, one hydrated salt wall, and a control wall. The two paraffin walls contained cellulose enhanced with RT27 PCM at concentrations of 10% (herein referred to as the “10% RT27 wall”) and 20% (herein referred to as the “20% RT27 wall”). The hydrated salt wall contained cellulose enhanced with TH29 PCM at a concentration of 10% (herein referred to as the “10% TH29 wall”). The fourth wall, the control wall, contained regular, unmodified cellulose insulation.

In the third series of tests, four walls were tested: three hydrated salt walls and a control wall. Two of the hydrated salt walls contained cellulose enhanced with TH24 PCM at concentrations of 10% (herein referred to as the “10% TH24 wall”) and 20%

(herein referred to as the “20% TH24 wall”). The third hydrated salt wall contained cellulose enhanced with TH29 PCM at a concentration of 20% (herein referred to as the “20% TH29 wall”). The fourth wall, the control wall, contained regular, unmodified cellulose insulation.

In the fourth series of tests, four walls were tested: two powdered paraffin walls, one eutectic paraffin/salt wall, and a control wall. The two powdered paraffin walls contained cellulose enhanced with PX27 PCM at concentrations of 10% (herein referred to as the “10% PX27 wall”) and 20% (herein referred to as the “20% PX27 wall”). The eutectic paraffin/salt wall contained cellulose enhanced with SP25 PCM at a concentration of 20% (herein referred to as the “20% SP25 wall”). The final wall, the control wall, contained regular, unmodified cellulose insulation.

In the fifth series of tests, four walls were tested: two powdered paraffin walls, one liquid/solid paraffin wall, and a control wall. The two powdered paraffin walls contained cellulose enhanced with PX27 PCM at concentrations of 20% (herein referred to as the “20% PX27 wall”) and 40% (herein referred to as the “40% PX27 wall”). The paraffin wall contained cellulose enhanced with RT27 PCM at a concentration of 30% (herein referred to as the “30% RT27 wall”). The final wall, the control wall, contained regular, unmodified cellulose insulation. A summary of the five test series performed is given in Table 9.

Table 9. Summary of Tests Performed

Test Series	Test Wall #1	Test Wall #2	Test Wall #3	Test Wall #4
TH29-F127	Control	TH29-F127	--	--
TH29 and RT27	Control	10% RT27	20% RT27	10% TH29
TH24 and TH29	Control	10% TH24	20% TH24	20% TH29
PX27 and SP25	Control	10% PX27	20% PX27	10% SP25
PX27 and RT27	Control	20% PX27	40% PX27	30% RT27

Dynamic Wall Simulator

Heat transfer performance testing was conducted using a dynamic wall simulator (Figure 11). The simulator was a cubic box designed to hold six 1.19 m x 1.19 m (47 in x 47 in) walls. A heat source of six 200W light bulbs was placed equidistant at the center of the simulator's interior (Figure 12). Two 80 mm x 80 mm (3 in. x 3 in.) fans were placed inside the simulator to assure a more uniform temperature distribution within the box, as shown in Figure 13.

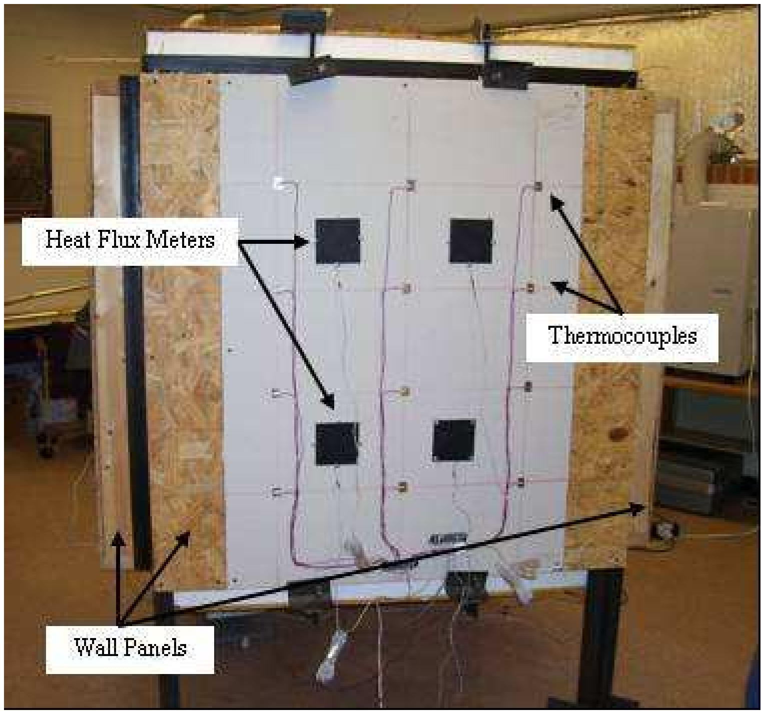

Figure 11. Exterior View of Dynamic Wall Simulator

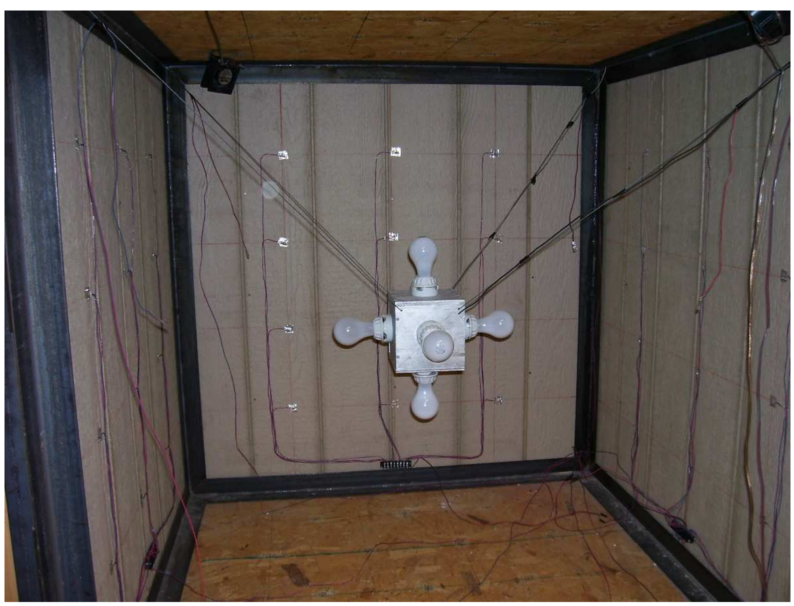

Figure 12. Interior View of Dynamic Wall Simulator

Figure 13. Interior Fan

The output from the heat source was varied and controlled with a digital timer and dimmer switch (Figure 14) to simulate daily exposure of walls to the sun. Using this configuration, the interior of the simulator represented the exterior of a typical building. Since the simulator was housed in an air-conditioned laboratory, the exterior of the simulator represented the interior conditioned space.

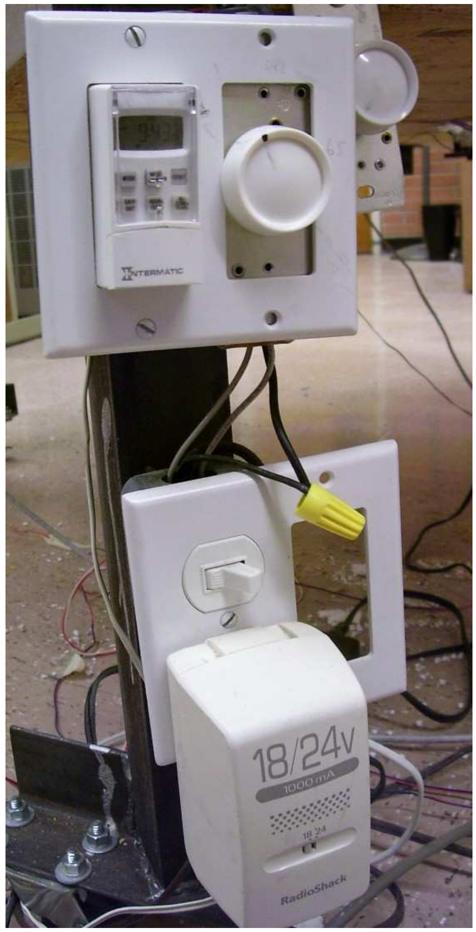

Figure 14. Digital Timer and Dimmer Switch

The three test walls and one control wall in each test series were tested at varied maximum interior wall surface temperatures in 6- to 8-hour heating cycles. The maximum interior wall surface temperature was varied to simulate different exposures to the sun. In other words, a higher interior wall surface temperature would model a hotter, sunnier summer day. The maximum interior wall surface temperature was set by adjusting the intensity of the heating source (i.e., the light bulbs) using the dimmer switch. A heating cycle of 8 hours was chosen based on results from previous field tests on south facing walls performed at the University of Kansas [26]. Shorter heating periods of 6 and 7 hours were tested to determine the effects heating length on peak heat flux reduction.

Thermocouples arranged on the interior and exterior surfaces of the frame walls measured surface temperatures. Thermocouples were also used to measure the interior and exterior air temperatures. Twelve type T thermocouples were affixed to each wall surface, as shown in Figure 15, and covered with aluminum tape to assure good contact between the thermocouple and the wall surface and to minimize the effects of radiation. Each set of 12 thermocouples was connected in parallel to measure one average wall surface temperature.

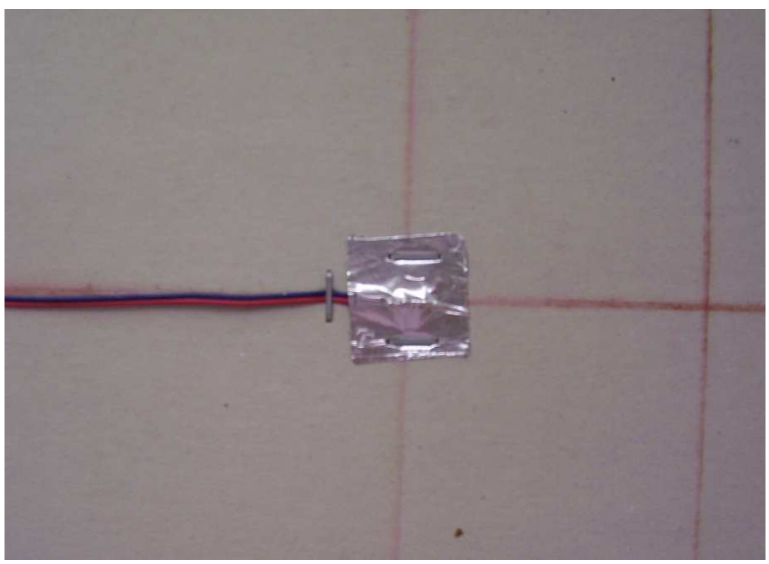

Figure 15. Thermocouples Shielded by Aluminum Tape

Four heat flux meters were installed on the exterior of each wall (wallboard side, over the insulated cavity) to measure the heat transfer rate through each wall (Figure 16).

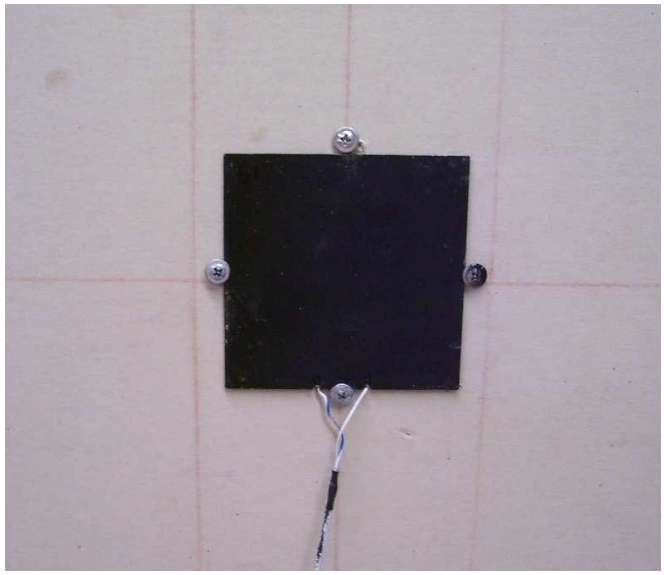

Figure 16. Heat Flux Meter

Table 10 shows the range and accuracy of the heat flux meters and thermocouples.

Table 10. Heat Flux Meter and Thermocouple Data

Sensor	Range	Accuracy (deviation)
Heat Flux Meter	0 - 3.1 x 10^5 W/m^2 (98.3 MBtu/hr ft^2)	2%
Type T Thermocouple	-18 - 93℃ (0 - 200℉)	0.6℃ (1℉)

Both thermocouples (T/C) and heat flux meters (HFM) were placed on the exterior wall surface in an evenly distributed arrangement over the insulated cavity only (Figure 17). Thermocouples were placed on the interior wall surface in the same positions as the thermocouples on the exterior wall surface.

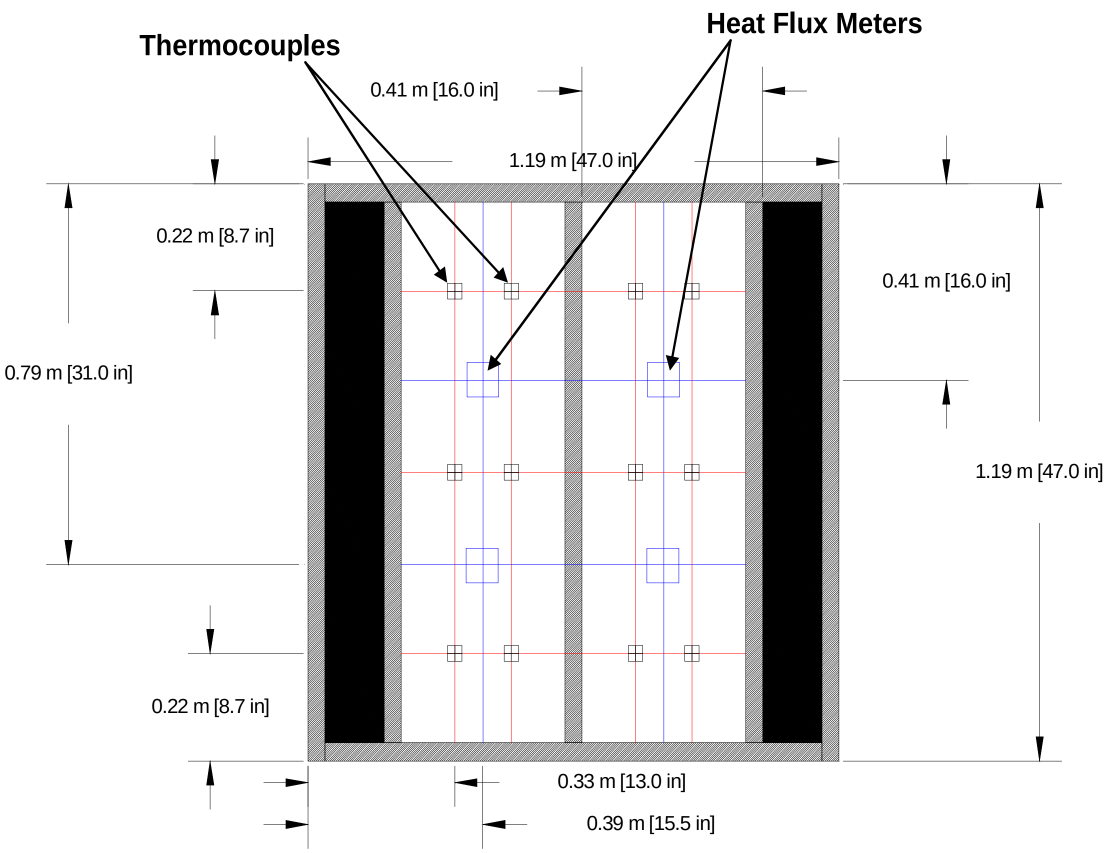

Figure 17. Arrangement of Thermocouples and Heat Flux Meters on Exterior Wall Surface

Data were collected by means of a data acquisition system every 20 seconds for 24-hour periods. The data acquisition system used was the Agilient 34970A data logger (Figure 18). A schematic of the arrangement of the data acquisition system is shown in Figure 19.

Figure 18. Agilient 34970A Data Logger

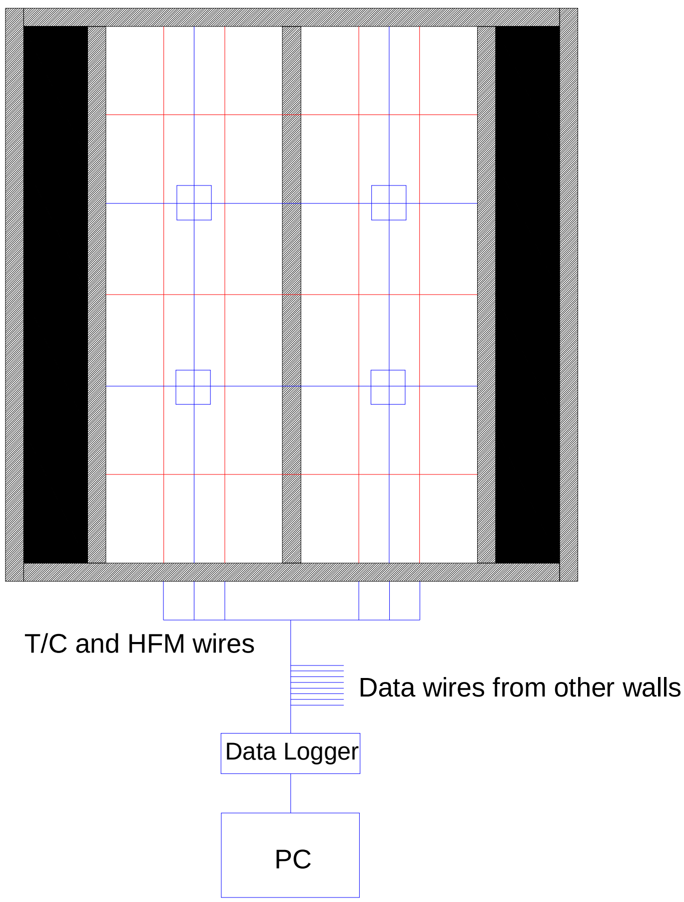

Figure 19. Schematic of the Arrangement of the Data Acquisition System

Data collected were reduced and organized using electronic spreadsheets. All temperatures and heat fluxes were averaged hourly from data collected at 20-second intervals. The average peak heat flux and total heat flow over the test period were calculated for each wall. The peak heat flux and total heat flow in each wall with PCM-enhanced insulation was compared to the control wall. Thermal performances of the walls were evaluated by comparing how well the insulation mixture reduced the peak heat flux and total heat flow compared to the control wall.

The walls were tested over several 24-hour periods. The walls were in a state of cooling at the beginning of each test. The heat source was turned on and the walls were heated for periods of 6 to 8 hours for each PCM cellulose mixture. The heat source was then turned off and the walls were allowed to cool. In many tests, the maximum wall surface heating temperature was varied slightly to determine if thermal performance was dependent on temperature range.

CHAPTER V

RESULTS AND DISCUSSION

Test Results

TH29-F127 Tests

A three-day test was performed on the TH29-F127 wall by heating both the test wall and the control wall to a maximum temperature of approximately 62°C (143.6°F) for 8 hours and then allowing the walls to cool down for 16 hours, then repeating the cycle of heating and cooling for two more days. The heat fluxes were measured and recorded every 20 seconds and averaged on an hourly basis. The averages are shown in Table 11. In the tabulated test results, each test number refers to an individual test performed in a 24-hour cycle.

Table 11. Comparison of Averaged Peak Heat Flux between the TH29-F127 Wall and Control Wall

	Max Temp *		Control		10% TH29-F127		
Test #	°C	°F	W/m^2	$Btu/hr{\cdot}ft^2$	W/m^2	$Btu/hr{\cdot}ft^2$	Reduction
1	62.0	143.6	19.50	6.18	19.96	6.33	-2.4%
2	62.0	143.7	19.59	6.21	19.87	6.30	-1.4%
3	62.2	144.0	19.81	6.28	20.16	6.39	-1.8%

* Max Temp is the maximum wall surface temperature in the interior of the simulator.
The interior of the simulator represented the exterior of a typical building.

The averaged hourly heat fluxes were graphed over one 24-hour test period as shown in Figure 20. In Figure 20 and similar graphs, the lines represent values of heat flux from the interior of the simulator to the exterior, across each wall. In this test, the interior of the simulator was heated to an average maximum temperature of 62.0°C (143.7°F). In Figure 20, during most of the heating cycle, the TH29-F127 wall had an average heat flux that followed very closely to that of the control wall. In other words, no significant difference in the heat flux was detected between the TH29-F127 wall and the control wall. As well, the curves of these walls show no apparent time shift of the peak heat flux, that is, the peak of the TH29-F127 curve does not occur later in time than the control curve. Also evident during the cool down phase, the heat flux in the TH29-F127 wall was actually lower than that of the control wall. These results show that little energy was stored in the TH29-F127 and, subsequently, little heat was released during the cool down period. It was concluded that much of the salt may not have solidified during the cool down period. This was supported by the observation that during the heating cycle, the salt absorbed little energy in phase change from solid to liquid. This was typical in most tests performed with the TH29-F127.

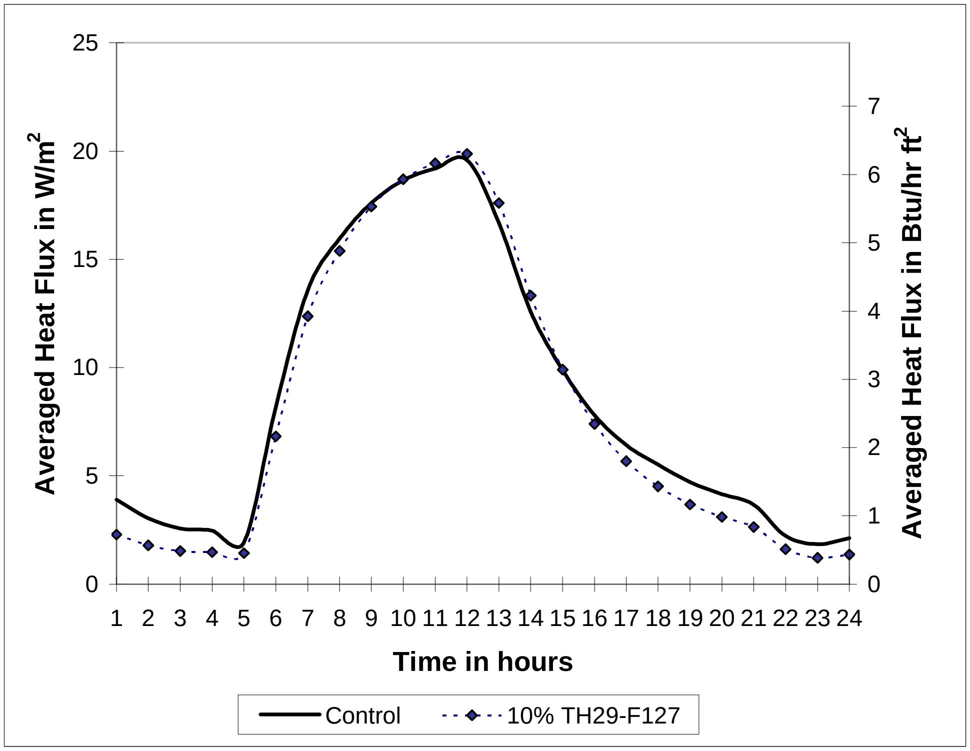

Figure 20. Averaged Heat Flux for TH29-F127 Test

To actually see the effects of temperature on the TH29-F127, a small sample was heated. While the TH29-F127 never actually melted, it did become “mushy” and “greasy” if agitated. Over time, the TH29-F127 absorbed moisture from the air and began to “sweat” as shown in Figure 21. The sample was then cooled down, and while it was uncertain if the temperature ever reached a point below 29ºC (84.2ºF), the sample seemed to stay in the same state (i.e., mushy, greasy, and wet). It is unknown what condition the TH29-F127 may have been in under similar conditions while mixed in the cellulose.

Figure 21. Partially Melted TH29-F127 PCM

It should be noted that even though the TH29-F127 test results showed no thermal storage benefit due to phase change, calculations of the total daily heat flow through the walls show that TH29-F127 wall transferred approximately 6.9% less heat overall than the control wall. In general, the TH29-F127 appeared to absorb water and became ineffective as a thermal storage material. To determine the effect of water absorption on the thermal storage performance of the un-encapsulated hydrated salt, further investigation was made with the TH29 PCM in the second series of tests.

TH29 and RT27 Tests

In this test series, paraffin-based PCM RT27 was tested in concentrations of 10% and 20%. The un-encapsulated hydrated salt PCM, TH29, was tested in a concentration of 10%. A total of thirteen daily tests were performed. Heat fluxes and wall surface temperatures were recorded every 20 seconds and averaged hourly. The averaged heat fluxes were graphed over the test period as shown in Figure 22. In this test, the interior of the simulator was heated to an average maximum temperature of 57.7°C (136°F). In Figure 22, for the first several hours of the heating cycle, which began at hour 9 (the first 8 hours corresponded to the cool down period of a previous heating cycle), the 10% RT27 wall and 20% RT27 wall (both paraffin walls) had much lower average heat fluxes compared to the control wall with a more pronounced reduction in the 20% RT27 wall. The curves of these walls show a lower peak heat flux (5.1% for the 10% RT27 wall and 10.3% for the 20% RT27 wall) and a time shift of the peak. The 10% TH29 wall performed similarly to the control wall until, partway through the heating cycle, the hydrated salt wall began to transfer more heat than the control wall, leading to a 9.7% increase in peak heat flux. This can be seen in Figure 22, as the curve of the 10% TH29 wall is above the curve of the control wall. As was typical in most tests performed, both of the paraffin-enhanced walls had lower peak heat fluxes when compared to the control wall. With both paraffin-enhanced walls, there was also a noticeable shift in peak (approximately 2 hours in the test shown in Figure 22), but only a slight shift in the 10% TH29 wall.

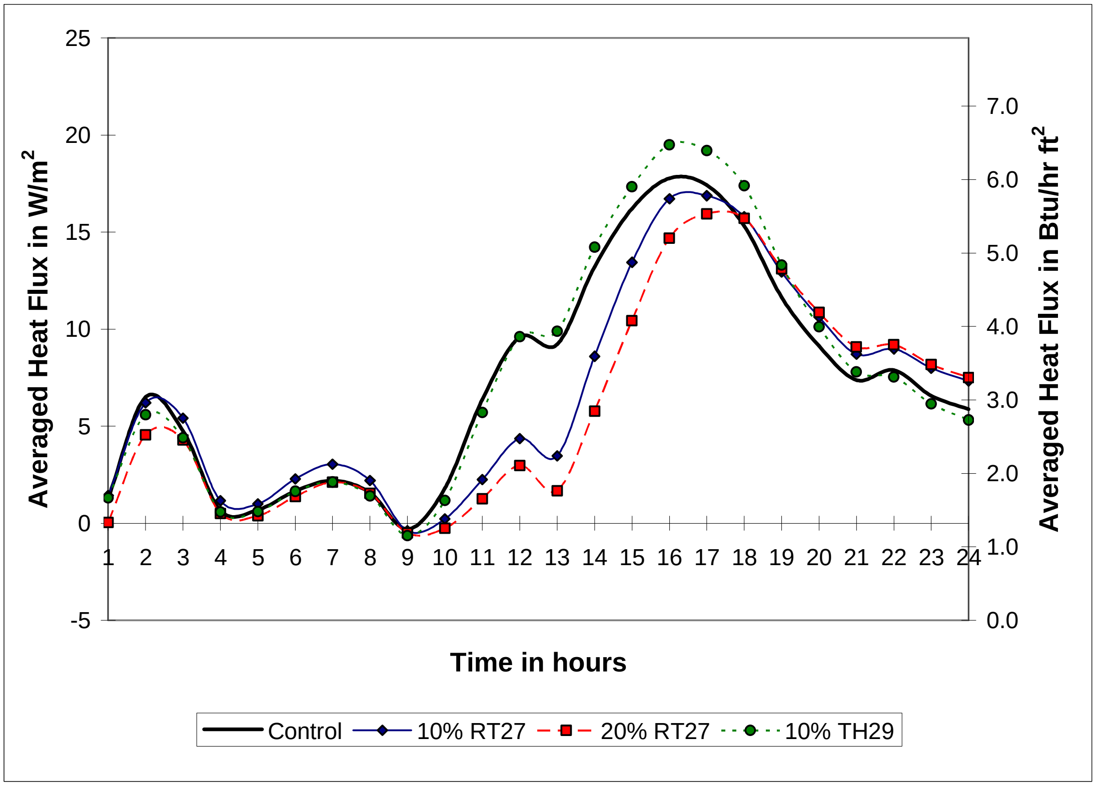

Figure 22. Averaged Heat Flux for RT27 and TH29 Test

As shown in Figure 22, the two walls with paraffin-enhanced insulation transferred energy at a lower rate than the control wall during the entire heating cycle (hours 9 through 17). During this time, the paraffin was changing phase from solid to liquid and absorbing energy adiabatically. When the heat source was turned off, these walls transferred more heat than the control wall throughout much of the cool down period. This was because the PCM-enhanced walls were rejecting the stored heat. This cycle of energy absorption and rejection repeated itself during consecutive tests. The paraffin walls not only reduced the peak heat flux, but also shifted the transfer of that heat to a later part of the "day."

In contrast, the 10% TH29 wall transferred the same amount of heat at the beginning and more toward the end of the heating cycle. This seems to indicate that the hydrated salt PCM did not absorb energy. This was likely because of the hydroscopic properties of the hydrated salt. That is, if used in an un-encapsulated form, the hydrated salt absorbed moisture as soon as it was exposed to moist air. This added moisture in the cellulose insulation allowed more heat to be conducted through the salt-enhanced wall than the control wall. The increased conductivity as a result of water absorption, coupled with the already higher conductivity of hydrated salt, resulted in a larger peak heat flux in the 10% TH29 than in the control wall. From these results, it is apparent that there was no thermal storage benefit from the hydrated salt PCM at this concentration.

Averaged peak heat fluxes for every test were tabulated and the percent peak reductions were calculated. The maximum peak heating temperature of the indoor wall surfaces (which represent the outdoor surface of a building wall) ranged from 42.3°C to 59°C (108°F to 138.2°F). Results of the peak heat flux measurements and calculated percent reduction are given in Table 12. The total average peak heat flux reduction was 5.7% for the 10% RT27 wall and 9.2% for the 20% RT27 wall. For 10% TH29 wall, there was an increase in peak heat flux of 7.3% on average. A summary of the comparison of peak heat flux and reduction in each wall is shown in Figures 23 and 24, respectively.

Table 12. Comparison of Averaged Peak Heat Flux and Percent Reduction in RT27 and TH29 Tests

	Max Temp*		**Control**		**10% RT27**			**20% RT27**			**10% TH29**		
Test #	℃	℉	W/m^2	$Btu/hr{\cdot}ft^2$	W/m^2	$Btu/hr{\cdot}ft^2$	Reduction	W/m^2	$Btu/hr{\cdot}ft^2$	Reduction	W/m^2	$Btu/hr{\cdot}ft^2$	Reduction
1	58.4	137.1	14.05	4.46	13.52	4.29	3.8%	13.55	4.30	3.6%	15.62	4.95	-11.2%
2	48.0	118.3	10.90	3.46	10.63	3.37	2.5%	10.69	3.39	1.9%	11.10	3.52	-1.9%
3	42.3	108.1	11.01	3.49	10.11	3.21	8.2%	9.15	2.90	17.0%	12.66	4.02	-14.9%
4	46.8	116.3	12.60	4.00	12.19	3.87	3.2%	11.64	3.69	7.6%	14.49	4.60	-15.0%
5	49.7	121.5	10.32	3.27	9.02	2.86	12.6%	8.64	2.74	16.3%	11.22	3.56	-8.7%
6	59.0	138.2	15.29	4.85	14.44	4.58	5.6%	14.57	4.62	4.7%	15.73	4.99	-2.9%
7	58.7	137.6	17.78	5.64	16.88	5.35	5.1%	15.94	5.06	10.3%	19.50	6.19	-9.7%
8	57.7	135.9	14.86	4.71	14.39	4.56	3.1%	13.95	4.43	6.1%	15.80	5.01	-6.4%
9	57.7	135.8	14.99	4.75	14.25	4.52	4.9%	14.09	4.47	6.0%	15.77	5.00	-5.2%
10	56.6	134.0	14.78	4.69	13.83	4.39	6.4%	13.16	4.17	11.0%	15.76	5.00	-6.6%
11	52.5	126.5	11.93	3.78	11.09	3.52	7.1%	10.47	3.32	12.2%	12.35	3.92	-3.5%
12	52.2	125.9	13.19	4.18	12.62	4.00	4.4%	12.17	3.86	7.7%	13.60	4.31	-3.1%
13	47.7	117.8	11.44	3.63	10.63	3.37	7.1%	9.73	3.09	15.0%	12.18	3.86	-6.5%
	Average		**13.32**	**4.22**	**12.58**	**3.99**	**5.7%**	**12.14**	**3.85**	**9.2%**	**14.29**	**4.53**	**-7.3%**

* Max Temp is the maximum wall surface temperature in the interior of the simulator.
The interior of the simulator represented the exterior of a typical building.

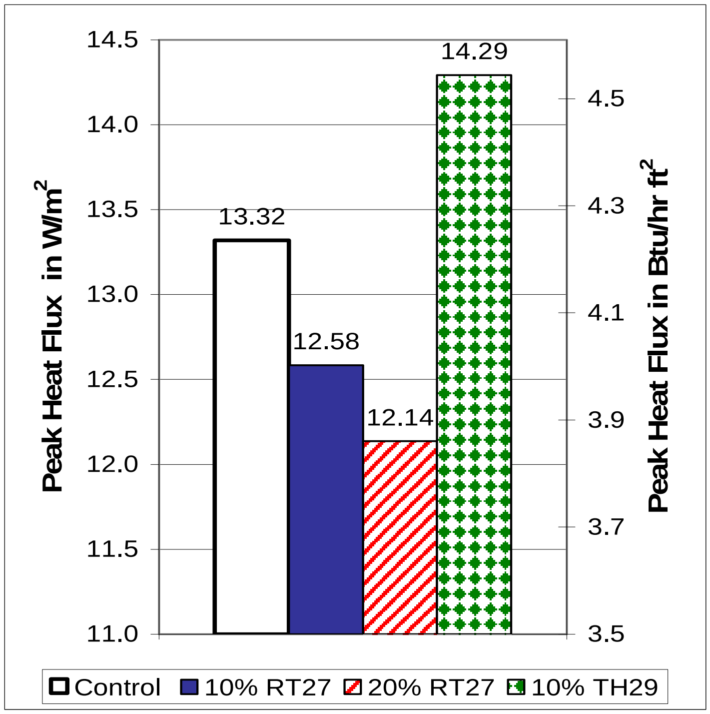

Figure 23. Comparison of Averaged Peak Heat Flux in RT27 and TH29 Tests

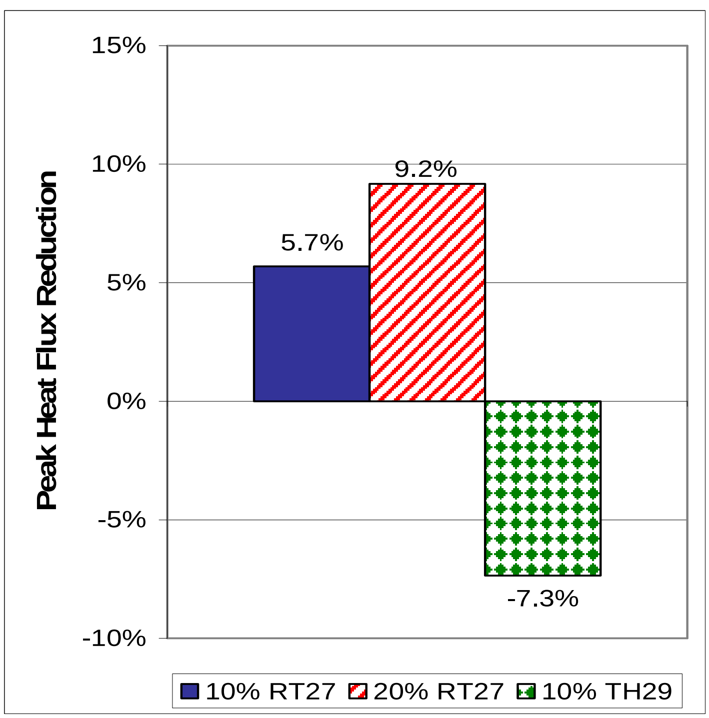

Figure 24. Comparison of Averaged Peak Heat Flux Reduction in RT27 and TH29 Tests

Thermal performance was also gauged by comparing the average total daily heat flow through each wall compared to the control wall. Since the 10% TH29 showed no apparent heat storage benefit (i.e., did not reduce the peak heat flux) in this application, as discussed previously, the total daily heat flow of the hydrated salt wall was not included in this analysis. The average total daily heat flow was calculated by integrating the hourly heat flux over the 24-hour period. Eleven 24-hour tests were performed in this experiment. The 24-hour average total daily heat flow for every test was tabulated and the percent total daily heat flow reduction was calculated. The maximum heating temperature on the interior wall surfaces ranged from 47.7°C to 58.7°C (117.8°F to 137.6°F). Results of the total daily heat flow measurements and calculated percent reduction are given in Table 13. The average total daily heat flow reduction was 0.6% for the 10% RT27 wall and 1.2% for the 20% RT27 wall. Table 13 includes only tests that were 24-hours in duration. A summary of the comparison of total daily heat flow and reduction in each paraffin wall is shown in Figures 25 and 26, respectively.

Table 13. Comparison of Averaged Total Daily Heat Flow and Percent Reduction between the Control and RT27 Test Walls

	Max Temp *		**Control**		**10% RT27**			**20% RT27**		
Test #	℃	℉	W/m ^{2}·day	Btu/day·ft^2	W/m^2·day	Btu/day·ft^2	Reduction	W/m^2·day	Btu/day·ft^2	Reduction
1	58.4	137.1	167.68	53.18	169.17	53.66	-0.9%	175.99	55.82	-5.0%
7	58.7	137.6	174.45	55.33	160.72	50.98	7.9%	140.50	44.56	19.5%
8	57.7	135.9	156.67	49.69	157.75	50.03	-0.7%	161.45	51.21	-3.1%
9	57.7	135.8	163.63	51.90	163.95	52.00	-0.2%	167.58	53.15	-2.4%
10	56.6	134	180.43	57.23	183.05	58.06	-1.5%	184.68	58.58	-2.4%
11	52.5	126.5	131.90	41.84	129.56	41.09	1.8%	130.73	41.47	0.9%
12	52.2	125.9	147.32	46.73	149.92	47.55	-1.8%	151.14	47.94	-2.6%
13	47.7	117.8	142.88	45.32	142.94	45.34	0.0%	138.14	43.81	3.3%
	Average		**158.12**	**50.15**	**157.13**	**49.84**	**0.6%**	**156.27**	**49.57**	**1.2%**

* Max Temp is the maximum wall surface temperature in the interior of the simulator. The interior of the simulator represented the exterior of a typical building.

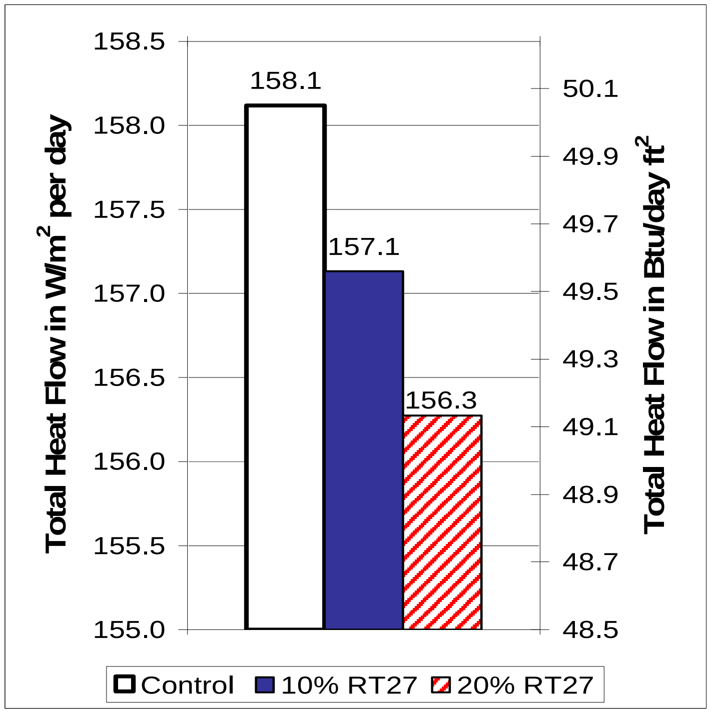

Figure 25. Comparison of Averaged Total Daily Heat Flow in RT27 and TH29 Tests

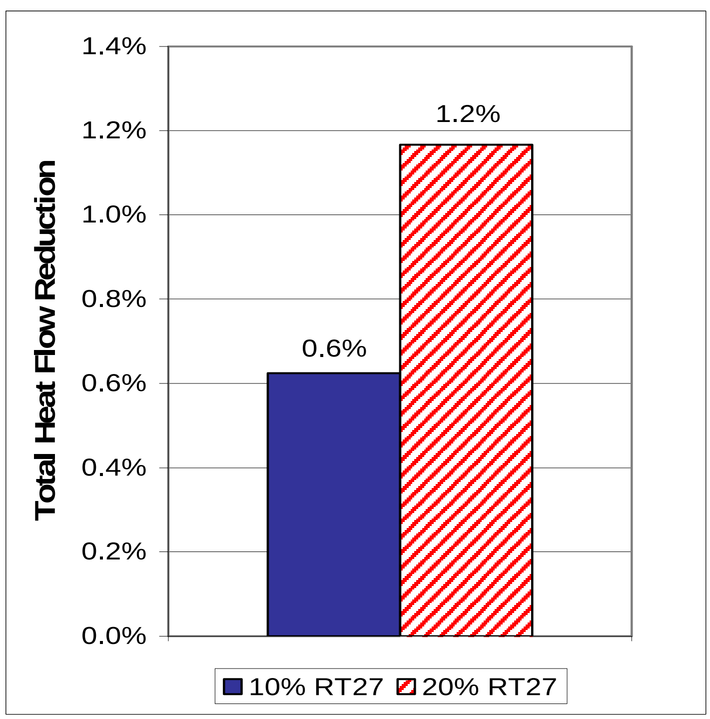

Figure 26. Comparison of Averaged Total Daily Heat Flow Reduction RT27 and TH29 Tests

It should be noted that the daily heat flow reductions from these simulator tests were lower that what may be observed in a building under full weather conditions because the interior of the simulator never cooled down to a temperature that was lower than the temperature in the laboratory. In reality, the exterior wall of a building may cool to a temperature lower than the interior wall temperature because of cooler outdoor (ambient) temperature or night sky radiation. If the exterior surface of a wall is cooler than the interior surface, some of the heat stored in the wall would be rejected to the cooler exterior, thus further reducing the energy transferred into the conditioned space. Potentially, the daily heat flow reductions measured in these tests may have been larger if the temperature inside the simulator was cooler than outside the simulator.

The peak reduction vs. indoor wall surface temperature for each test was plotted to determine if there was a performance trend based on wall temperature. These results are shown in Figure 27. It can be seen that the 20% RT27 wall performed best at the lower range of maximum heating temperature, but as the maximum wall temperature was increased, the performance decreased. Likewise, the 10% RT27 wall performed better at the lower temperatures, but the average heat flux was relatively stable throughout the temperature range. This reduction in peak heat flux may be the result of the quick melting of the PCM at the higher temperatures. In other words, much of the PCM may have melted and could no longer absorb heat. At mid-range to lower maximum temperature, the reduction was more pronounced likely because the PCM was melting at a slower rate and continued to absorb heat throughout the heating period. The decreased performance at higher temperatures may represent that on hotter summer days the effectiveness of the PCM decreases. This indicates that the PCM may perform better in milder climates or in walls with a lesser exposure to the sun's radiation.

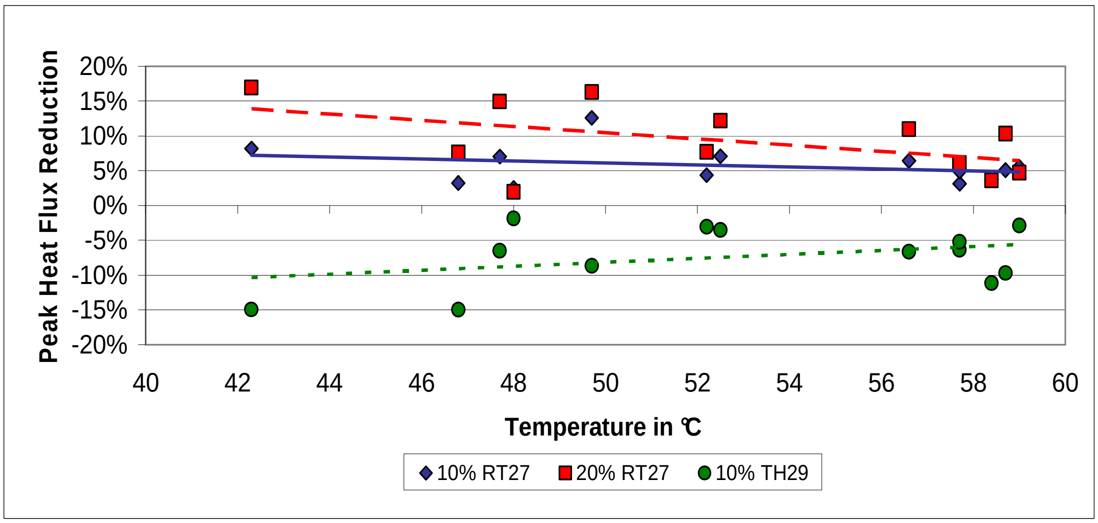

Figure 27. Comparison of Peak Heat Flux Reduction for the RT27 and TH29 Tests

To verify that the 10% TH29 wall had no thermal storage benefit in this test series, the performance of that wall was plotted, as shown in Figure 27. As expected, the 10% TH29 wall performed poorly at all temperatures and actually transferred more heat than the control wall throughout the temperature range likely the result of the increased conductivity in the moisture and in the TH29 PCM. A point of interest regarding the performance of the 10% TH29 wall is that the performance actually "improved" as the temperature increased. This may be the result of the evaporation of water that was absorbed by the TH29 PCM. The higher temperatures may have facilitated some of the liquid water to change to water vapor and thus absorbed energy in the phase change process. Even with this slight recovery of performance, the un-encapsulated 10% TH29 PCM did not provide any thermal storage benefit and cannot be considered feasible in this application.

The total daily heat flow reduction vs. wall temperature for each test was plotted to determine if there was a performance trend based on wall temperature. This analysis was performed on the RT27 walls only since the un-encapsulated 10% TH29 PCM was eliminated as a thermal storage medium in this application. The results are shown in Figure 28. From these results, it can be seen that both the 10% RT27 wall and the 20% RT27 wall gave a small reduction in total average daily flow when compared to the control wall, and as maximum heating temperature increased, the percent reduction also increased slightly. These reductions of daily heat flow may be smaller than what might have been measured in an actually building wall because of the limitations of the simulator. The interior temperature in the simulator never fell to a temperature below the conditioned space outside of the simulator. In reality, heat is rejected to the cooler outdoor environment due to cooler air temperatures or night sky radiation. This heat rejection to the cooler outdoor environment would reduce the total daily heat flow transferred into the conditioned space and increase the percent reduction in total heat flow. Although the simulator tests did not providing significant reductions in the total daily heat flow, the RT27 PCM did contribute to the overall the reduction in energy transferred (peak and total) into the conditioned space.

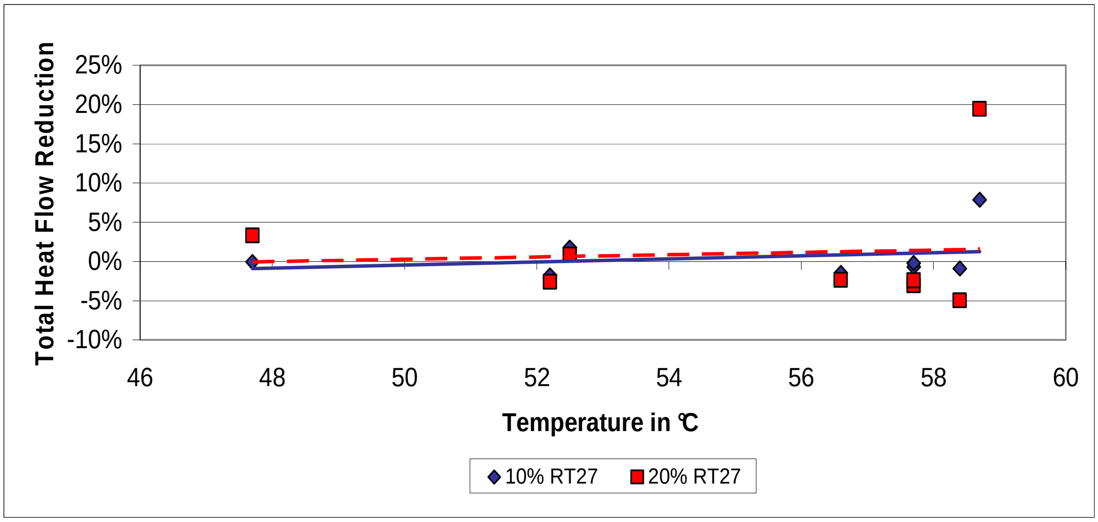

Figure 28.

Comparison of Averaged Total Daily Heat Flow Reduction for RT27 Walls

TH24 and TH29 Tests

The poor performance of 10% TH29 wall led to the investigation of the un-encapsulated hydrated salt PCM with difference concentrations and melting temperatures. In this test series, un-encapsulated hydrated salt PCM, TH29, was tested in a concentration of 20% and un-encapsulated hydrated salt PCM, TH24, was tested in concentrations of 10% and 20%. A total of ten daily tests were performed. Heat flux and wall surface temperatures were recorded and averaged hourly. The averaged heat fluxes were graphed over the test period as shown in Figure 29. In this example, the interior of the simulator was heated to an average maximum temperature of 53.2°C (127.8°F). In Figure 29, for the three hours of the heating cycle, the heat flux in the hydrated salt walls followed very closely to the heat flux in the control wall. Between hours 8 and 13 of the heating cycle, the hydrated salt walls transferred more heat to the cooler environment. The 10% TH24 wall transferred less heat than either the 20% TH24 wall or the 20% TH29 wall. The heat flux curves of these walls show a higher peak heat flux (23% higher for the 10% TH24 wall, 37% higher for the 20% TH24, and 33% higher for the 20% TH29 wall) and no apparent time shift of the peak. During the cool down period (beginning at hour 13), the hydrated salt walls continued to transfer more heat than the control wall until most of the heat was dissipated from the interior of the simulator and the curves leveled off near hour 20. As was typical in all the tests performed, the control wall had a lower peak heat flux than any of hydrated salt walls by a large margin and no significant time shift of peak.

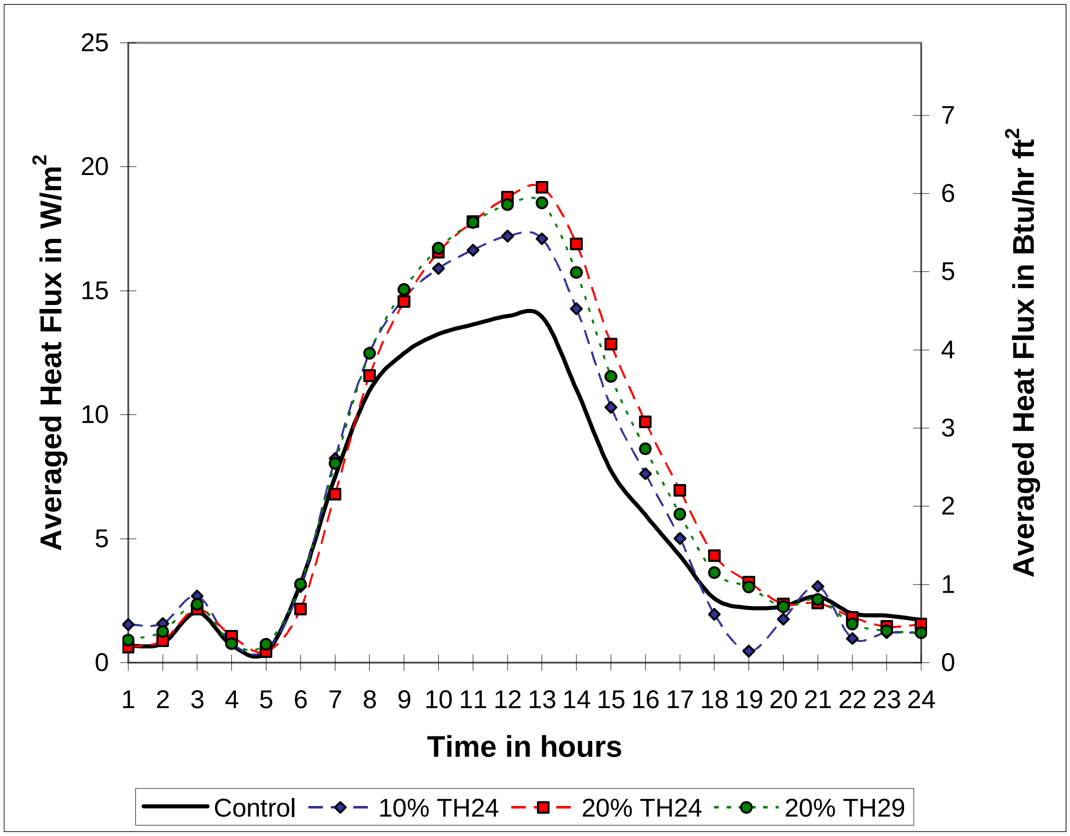

Figure 29. Averaged Heat Flux for TH24 and TH29 Test

As was seen in the 10% TH29 tests above, the hydrated salt walls in this test transferred the same amount of heat at the beginning and more heat toward the end of the heating cycle. This again indicated that the hydrated salt PCM did not absorb energy, but rather conducted more heat through the wall likely because of added moisture in the PCM-enhanced cellulose insulation. Tabulated results of peak heat flux for all test performed in this series are shown in Table 14.

Table 14. Comparison of Averaged Peak Heat Flux and Percent Reduction in the TH24 and TH29 Tests

	Max Temp *		Control		10% TH24			20% TH24			20% TH29		
Test #	℃	℉	W/m^2	$Btu/hr{\cdot}ft^2$	W/m^2	$Btu/hr{\cdot}ft^2$	Reduction	W/m^2	$Btu/hr{\cdot}ft^2$	Reduction	W/m^2	$Btu/hr{\cdot}ft^2$	Reduction
1	52.9	127.2	12.71	4.03	14.96	4.75	-17.7%	16.31	5.17	-28.2%	15.37	4.87	-20.9%
2	65.2	149.3	20.04	6.36	22.29	7.07	-11.2%	25.08	7.95	-25.1%	23.89	7.58	-19.2%
3	50.0	122.0	12.62	4.00	14.69	4.66	-16.4%	15.38	4.88	-21.8%	15.08	4.78	-19.4%
4	53.2	127.8	13.97	4.43	17.20	5.46	-23.1%	19.17	6.08	-37.2%	18.54	5.88	-32.7%
5	53.6	128.4	13.97	4.43	16.60	5.27	-18.8%	18.34	5.82	-31.3%	17.77	5.64	-27.2%
6	53.9	128.9	13.85	4.39	16.49	5.23	-19.0%	18.11	5.74	-30.7%	17.64	5.59	-27.3%
7	56.8	134.2	15.62	4.95	18.41	5.84	-17.9%	20.70	6.57	-32.5%	19.52	6.19	-25.0%
8	59.5	139.2	16.88	5.36	19.86	6.30	-17.7%	22.10	7.01	-30.9%	20.81	6.60	-23.3%
9	60.6	141.0	16.14	5.12	18.99	6.02	-17.6%	21.01	6.66	-30.1%	20.33	6.45	-26.0%
10	64.8	148.7	18.10	5.74	21.16	6.71	-16.9%	23.63	7.50	-30.6%	22.47	7.13	-24.1%
	Average		**15.39**	**4.88**	**18.07**	**5.73**	**-17.6%**	**19.98**	**6.34**	**-29.9%**	**19.14**	**6.07**	**-24.5%**

* Max Temp is the maximum wall surface temperature in the interior of the simulator. The interior of the simulator represented the exterior of a typical building.

As shown in Table 14, in all tests performed, each hydrated salt wall had a higher average peak heat flux than the control wall. As an average of all test performed, the 10% TH24 wall had a higher peak heat flux by 17.6%, the 20% TH24 had a higher peak heat flux by 29.9%, and the 20% TH29 wall had a higher peak heat flux of 24.5% than the control wall. These results reinforce the previous conclusion that there was no thermal storage benefit from the hydrated salt PCM in any concentration or melting point. It is interesting to note that the TH29 with a melting temperature of 29°C (84.2°F) performed better than the TH24 with its melting temperature of 24°C (75.2°F). This may reflect the possibility of a relationship between melting point temperature and performance of the hydrated salt PCM.

PX27 and SP25 Tests

In the fourth test series, the powdered paraffin PCM PX27 was tested in concentrations of 10% and 20% and the eutectic salt/paraffin PCM SP25 was tested in a concentration of 10%. A total of eleven daily tests were performed. Heat flux and wall surface temperatures were recorded every 20 seconds and averaged hourly. The averaged heat fluxes were graphed over the test period as shown in Figure 30. In this example, the interior of the simulator was heated to an average maximum temperature of 55.5°C (132°F). In Figure 30, for the first several hours of the heating cycle which began at hour 4 (the first hours correspond to the cool down period of a previous cycle), the 10% PX27 wall and 20% PX27 wall (both paraffin walls) had much lower average heat fluxes compared to the control wall, with a more pronounced reduction in the 20% PX27 wall. Near the end of the heating cycle (hour 12), both PX27 walls had a heat flux very close to the control wall. Just after the heat source was turned off, the heat fluxes of both PX27 walls continued to climb and reached a slightly higher peak heat flux than the control wall. The curves of these walls show a higher peak heat flux of 0.9% for the 10% PX27 wall and 1.7% for the 20% PX27 wall, but they both show a small time shift of the peak (approximately 30 – 60 minutes). The 10% SP25 wall had a lower heat flux during the first part of the heating cycle when compared to the control wall until, partway through the heating cycle, the 10% SP25 wall began to transfer significantly more heat than the control wall, leading to a 25% increase in peak heat flux. This can be seen in Figure 30, as the curve of the 10% SP25 wall is well above the curve of the control wall. As was typical in most tests performed, both of the PX27-enhanced walls had slightly higher peak heat fluxes than the control wall and the 10% SP25 wall had a largely higher peak heat flux than the control wall.

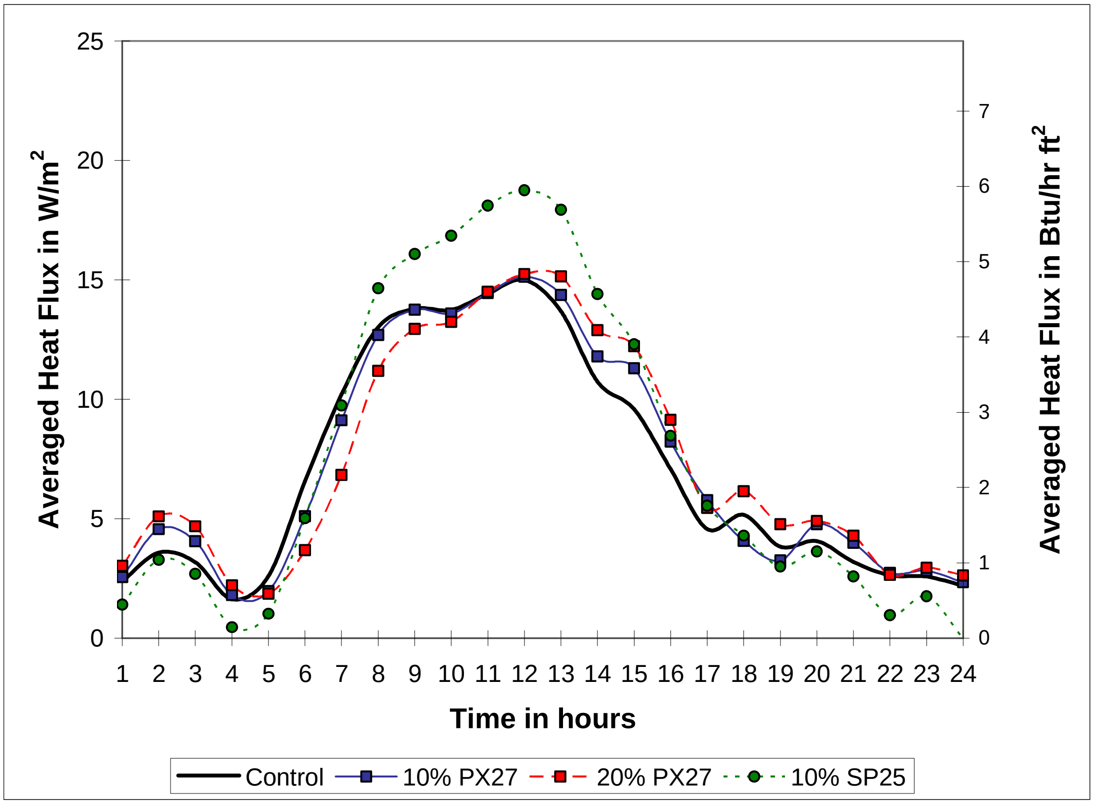

Figure 30. Averaged Heat Flux for PX27 and SP25 Test

As shown in Figure 30, the two walls with PX27-enhanced insulation transferred heat at a lower rate than the control wall during most of the heating cycle (hours 4 through 11). During this time, the PX27 was changing phase from solid to liquid and absorbing energy adiabatically. When the heat source was turned off, these walls transferred more heat than the control wall throughout much of the cool down period as it rejected the stored heat. However, unlike the RT27 paraffin PCM, the PX27 material did not store enough energy to reduce the peak heat flux. This indicated that the PX27 material was performing as a thermal storage device, but that there might not have been enough PCM in the cellulose to absorb a large enough amount of heat to provide thermal storage benefit. These results served to verify an observation made during the development of the PX27-enhanced walls. While the PX27 powdered paraffin-based PCM was easily mixed into the cellulose insulation, the powdered material was very difficult to keep well distributed during the installation of the insulation into the wall. As the insulation was being agitated in the blower's hopper, much of the PX27 powder separated from the insulation and settled to the bottom. From this observation and the corresponding results, it appeared that the concentration of PCM was much less than the 10% and 20% proposed.

The 10% SP25 wall transferred slightly less heat at the beginning and significantly more toward the end of the heating cycle. This indicates that as previously seen with the TH24 and TH29 hydrated salt PCM, this material did not absorb energy. Again, this is likely because of the hydroscopic properties of the hydrated salt. Even while formulated with paraffin and other additives, the hydrated salt in the SP25 compound absorbed moisture and again conducted more heat through the SP25-enhanced wall than the control wall. The SP25 PCM has a higher conductivity that may have contributed to the rather large peak heat fluxes that were measured in all tests. From these results, it was apparent that there was no thermal storage benefit from the SP25 PCM.

Averaged peak heat fluxes for every test were tabulated and the percent peak reductions were calculated. The maximum peak heating temperature of the indoor wall surfaces (which represent the outdoor surface of a building wall) ranged from 47.4°C to 80.1°C (117.2°F to 176.2°F). Results of the peak heat flux measurements and calculated percent reduction are given in Table 15. The total average peak heat flux increase was 1.3% for the 10% PX27 wall, 3.2% for the 20% PX27 wall, and 26.3% for the SP25 wall.

Table 15. Comparison of Averaged Peak Heat Flux and Percent Reduction in the PX27 and SP25 Tests

	Max Temp *		Control		10% PX27			20% PX27			10% SP25		
Test #	℃	℉	W/m^2	$Btu/hr{\cdot}ft^2$	W/m^2	$Btu/hr{\cdot}ft^2$	Reduction	W/m^2	$Btu/hr{\cdot}ft^2$	Reduction	W/m^2	$Btu/hr{\cdot}ft^2$	Reduction
1	80.1	176.2	26.60	8.44	26.26	8.33	1.2%	28.37	9.00	-6.7%	33.69	10.69	-26.7%
2	79.9	175.9	28.35	8.99	27.64	8.77	2.5%	29.10	9.23	-2.6%	34.37	10.90	-21.2%
3	80.4	176.8	26.61	8.44	26.86	8.52	-0.9%	28.57	9.06	-7.4%	33.10	10.50	-24.4%
4	68.5	155.4	20.64	6.55	20.57	6.52	0.3%	21.39	6.78	-3.6%	25.68	8.14	-24.4%
5	55.5	131.9	14.99	4.76	15.13	4.80	-0.9%	15.25	4.84	-1.7%	18.75	5.95	-25.0%
6	56.2	133.1	14.38	4.56	14.49	4.60	-0.8%	14.83	4.70	-3.1%	18.60	5.90	-29.3%
7	48.6	119.4	12.37	3.92	12.54	3.98	-1.4%	11.05	3.50	10.7%	15.29	4.85	-23.6%
8	47.8	118.0	12.12	3.84	12.55	3.98	-3.5%	12.48	3.96	-3.0%	15.29	4.85	-26.2%
9	47.0	116.7	11.75	3.73	11.88	3.77	-1.0%	11.98	3.80	-1.9%	14.78	4.69	-25.8%
10	47.9	118.3	11.87	3.77	12.74	4.04	-7.3%	13.41	4.25	-13.0%	16.05	5.09	-35.2%
11	47.4	117.2	12.10	3.84	12.40	3.93	-2.5%	12.46	3.95	-3.0%	15.43	4.89	-27.5%
	Average		**17.44**	**5.53**	**17.55**	**5.57**	**-1.3%**	**18.08**	**5.73**	**-3.2%**	**21.91**	**6.95**	**-26.3%**

* Max Temp is the maximum wall surface temperature in the interior of the simulator. The interior of the simulator represented the exterior of a typical building.

Since the eutectic PCM, SP25, performed poorly as thermal storage media, no further investigation was pursued with hydrated salt PCMs in any form. In order to test the PX27 powdered paraffin, a higher concentration (40%) of the material was developed for testing. Great effort was taken to keep the powdered material in mixture with the cellulose insulation.

PX27 and RT27 Tests

In this test series, the powdered paraffin PX27 and the paraffin-based PCM RT27 were tested in much higher concentrations of 40% and 30% (by weight of the wallboard) respectively. A total of nine daily tests were performed. Heat flux and wall surface temperatures were recorded and averaged hourly. The averaged heat fluxes were graphed over a 24-hour test period as shown in the example (Figure 31). In this daily test, the interior of the simulator was heated to an average maximum temperature of 54.9°C (130.8°F). In Figure 31, throughout the heating cycle which began at hour 4, both SP27 walls and the 30% RT27 wall had a much lower average heat flux compared to the control wall. The heat flux curves of these walls show lower peak heat fluxes (13.7% for the 40% PX27 wall and 4.5% for the 30% RT27 wall) than the control wall and noticeable time shifts of peak. The 20% PX27 wall had a small increase in peak heat flux of 2.4%, but still had a shift in peak. As was typical in all tests performed, the 40% PX27 wall and the 30% RT27 wall had lower peak heat fluxes the control wall while the 20% PX27 wall had a higher peak heat flux than the control wall. With both PX27 walls and the RT27 wall, there was also a noticeable shift in peak of approximately 30 – 60 minutes (as shown in Figure 31) in all tests performed in this test series.

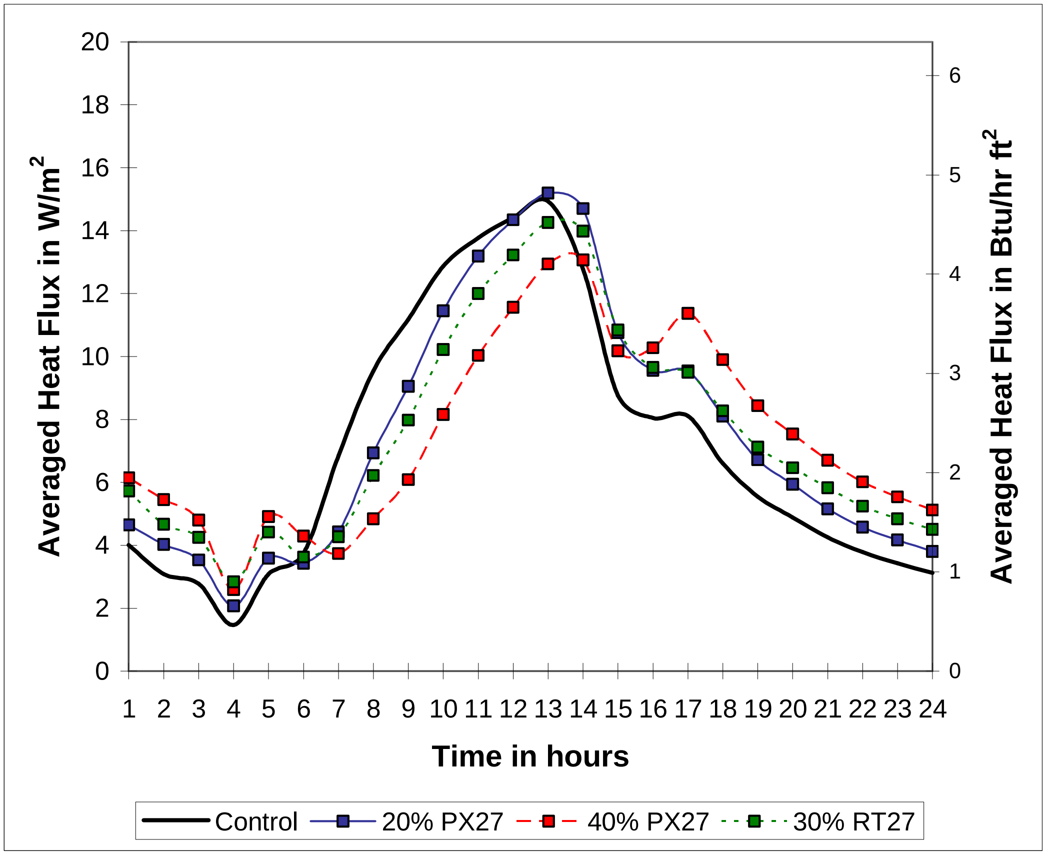

Figure 31. Averaged Heat Flux for PX27 and RT27 Test

Averaged peak heat fluxes for every test were tabulated and the percent peak reductions were calculated. The maximum peak heating temperature of the indoor wall surfaces (which represented the outdoor surface of a building wall) ranged from 54.2°C to 59.3°C (129.5°F to 138.8°F). Results of the peak heat flux measurements and calculated percent reduction are given in Table 16. The total average peak heat flux reduction was 9.3% for the 40% PX27 wall and 4.3% for the 30% RT27 wall. For 20% PX27 wall, there was a small increase in peak heat flux of 2.7% on average. A summary of the comparison of peak heat flux and reduction in each wall is shown in Figures 32 and 33, respectively.

Table 16. Comparison of Averaged Peak Heat Flux and Percent Reduction in the PX27 and RT27 Tests

	Max Temp *		Control		20% PX27			40% PX27			30% RT27		
Test #	℃	℉	W/m^2	$Btu/hr{\cdot}ft^2$	W/m^2	$Btu/hr{\cdot}ft^2$	Reduction	W/m^2	$Btu/hr{\cdot}ft^2$	Reduction	W/m^2	$Btu/hr{\cdot}ft^2$	Reduction
1	57.5	135.56	16.22	5.14	17.07	5.41	-5.3%	15.73	4.99	3.0%	15.84	5.02	2.4%
2	57.0	134.62	15.47	4.91	15.70	4.98	-1.4%	13.45	4.27	13.1%	14.38	4.56	7.1%
3	59.3	138.74	18.50	5.87	19.57	6.21	-5.8%	18.19	5.77	1.7%	18.36	5.82	0.8%
4	59.3	138.75	17.80	5.65	18.28	5.80	-2.7%	17.26	5.47	3.0%	17.43	5.53	2.0%
5	54.2	129.51	14.93	4.74	15.19	4.82	-1.7%	13.07	4.15	12.5%	14.26	4.52	4.5%
6	54.6	130.36	14.32	4.54	14.22	4.51	0.8%	11.69	3.71	18.4%	13.06	4.14	8.8%
7	54.9	130.77	14.69	4.66	15.04	4.77	-2.4%	12.67	4.02	13.7%	14.03	4.45	4.5%
	Average		**15.99**	**5.07**	**16.44**	**5.21**	**-2.7%**	**14.58**	**4.62**	**9.3%**	**15.34**	**4.86**	**4.3%**

* Max Temp is the maximum wall surface temperature in the interior of the simulator. The interior of the simulator represented the exterior of a typical building.

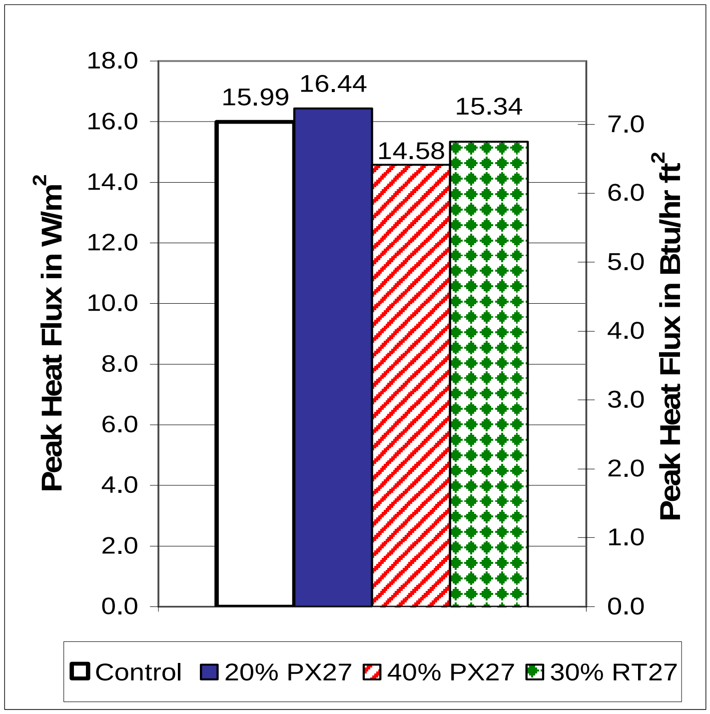

Figure 32. Comparison of Averaged Peak Heat Flux in PX27 and RT27 Tests

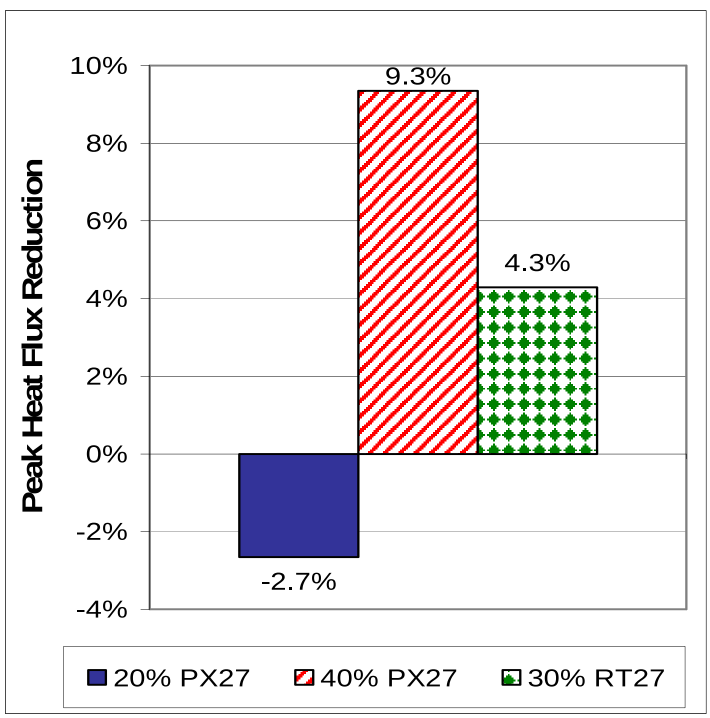

Figure 33. Comparison of Averaged Peak Heat Flux Reduction in PX27 and RT27 Tests

The total average daily heat flow through each wall was also compared to the control wall to gauge thermal performance. The total average daily heat flow was calculated by integrating the hourly heat flux over the 24-hour period. The daily average total heat flux for every test was tabulated and the percent total daily heat flow reduction was calculated. The maximum heating temperature on the interior wall surfaces ranged from 54.2°C to 59.3°C (129.5°F to 138.8°F). Results of the total daily heat flow measurements and calculated percent reduction are given in Table 17. There was a total daily heat flow increase of 4.5% for the 20% SP27 wall, a 5.1% increase for the 40% SP27, and a 5.4% increase for the 30% RT27 wall. While there was a reduction in peak heat flux in the 40% SP27 and the 30% RT27 walls, there was no reduction in total daily heat flow for any of the test walls. As discussed with the previous RT27 tests, the total daily heat flows in the test walls may potentially be lower than the control wall if measured under full weather conditions. Heat stored at night in the PCM test walls could be rejected to the cooler outdoor environment, thus decreasing the total daily heat flow transferred into the conditioned space. The simulator was not equipped to allow the interior temperature to fall below the temperature of the conditioned space, so any heat stored in the tests walls would be rejected to the cooler conditioned space. This limitation of the simulator may have caused larger total daily heat flows and lower percent reductions in the test walls when compared to the control wall.

Table 17. Comparison of Averaged Total Daily Heat Flow and Percent Reduction in the PX27 and RT27 Tests

	Max Temp *		Control		20% PX27			40% PX27			30% RT27		
Test #	℃	℉	$W/m^2 \cdot day$	$Btu/day \cdot ft^2$	$W/m^2 \cdot day$	$Btu/day \cdot ft^2$	Reduction	$W/m^2 \cdot day$	$Btu/day \cdot ft^2$	Reduction	$W/m^2 \cdot day$	$Btu/day \cdot ft^2$	Reduction
1	57.5	135.56	176.27	55.91	183.69	58.26	-4.2%	189.63	60.15	-7.6%	186.80	59.25	-6.0%
2	57.0	134.62	167.82	53.23	172.99	54.87	-3.1%	174.44	55.33	-3.9%	173.29	54.97	-3.3%
3	59.3	138.74	199.72	63.35	207.03	65.67	-3.7%	210.56	66.79	-5.4%	211.40	67.05	-5.8%
4	59.3	138.75	194.08	61.56	201.34	63.86	-3.7%	202.50	64.23	-4.3%	203.83	64.65	-5.0%
5	54.2	129.51	169.05	53.62	176.62	56.02	-4.5%	176.54	55.99	-4.4%	177.12	56.18	-4.8%
6	54.6	130.36	158.38	50.24	167.80	53.22	-5.9%	163.76	51.94	-3.4%	169.70	53.82	-7.1%
7	54.9	130.77	161.21	51.13	171.28	54.33	-6.2%	171.39	54.36	-6.3%	170.99	54.24	-6.1%
	Average		**175.22**	**55.58**	**182.96**	**58.03**	**-4.5%**	**184.12**	**58.40**	**-5.1%**	**184.73**	**58.59**	**-5.4%**

* Max Temp is the maximum wall surface temperature in the interior of the simulator. The interior of the simulator represented the exterior of a typical building.

The peak reduction vs. indoor wall surface temperature for each test was plotted to determine if there was a performance trend based on wall temperature. These results are shown in Figure 34. It can be seen that the 40% PX27 wall performed well at the lower range of maximum heating temperature, but as the maximum wall temperature was increased, the performance decreased significantly. Likewise, the 30% RT27 wall performed better at the lower temperatures, but as temperature increased, the average heat flux decreased at a lesser rate. For both of these walls, there was a reduction in peak heat flux throughout the temperature range, but the performance decreased with increase maximum heating temperature. This reduction decrease may be the result of the quick melting of the PCM at the higher temperatures. In other words, much of the PCM had melted and could no longer absorb heat. At lower maximum temperatures, the reduction was more pronounced likely because the PCM melted at a slower rate and continued to absorb heat throughout the heating period.

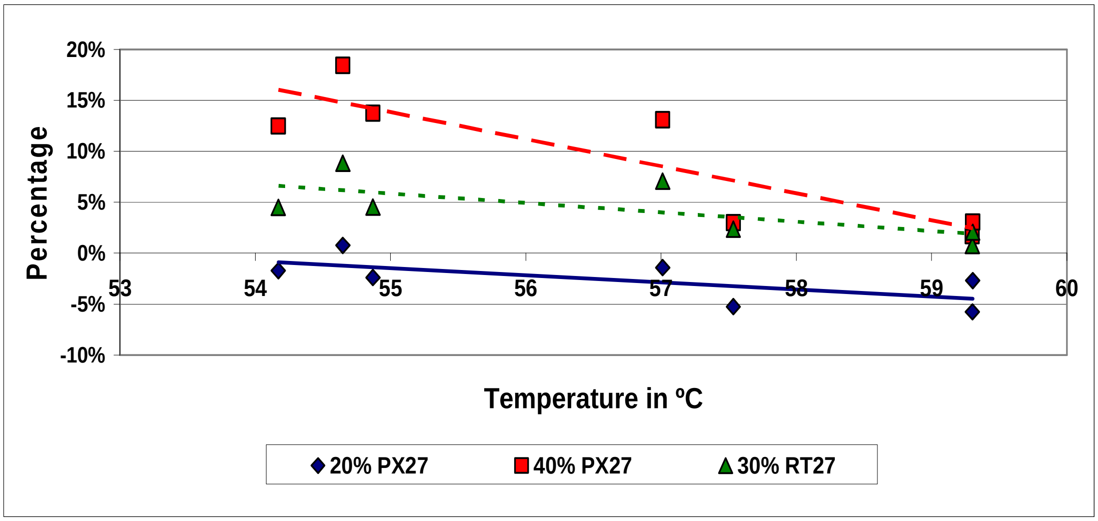

Figure 34. Comparison of Peak Heat Flux Reduction for PX27 and RT27 Tests

The performance of the 20% PX27 wall was also plotted in Figure 34. As expected from previous results, the 20% PX27 wall performed poorly at all temperatures by transferring more heat than the control wall throughout the temperature range. At the higher heating temperatures, the performance of the 20% PX27 wall decreased similarly to the 40% PX27 wall and likely for the same reason.

The total daily heat flow reduction vs. wall temperature for each test was plotted to determine if there was a performance trend based on wall temperature. From the results, shown in Figure 35, it can be seen that the test walls increased the total daily heat flow throughout the temperature range. Again, these total daily heat flow reductions may have been smaller than what would be expected in walls under full weather conditions. Positive total daily heat flow reductions may have been experienced if the interior of the simulator would have been allowed to cool to a temperature below the exterior conditioned space. While simulator tests did not provide significant reductions in the total daily heat flow, the 40% PX27 PCM and the RT27 PCM did contribute to the reduction in peak heat flux transferred into the conditioned space.

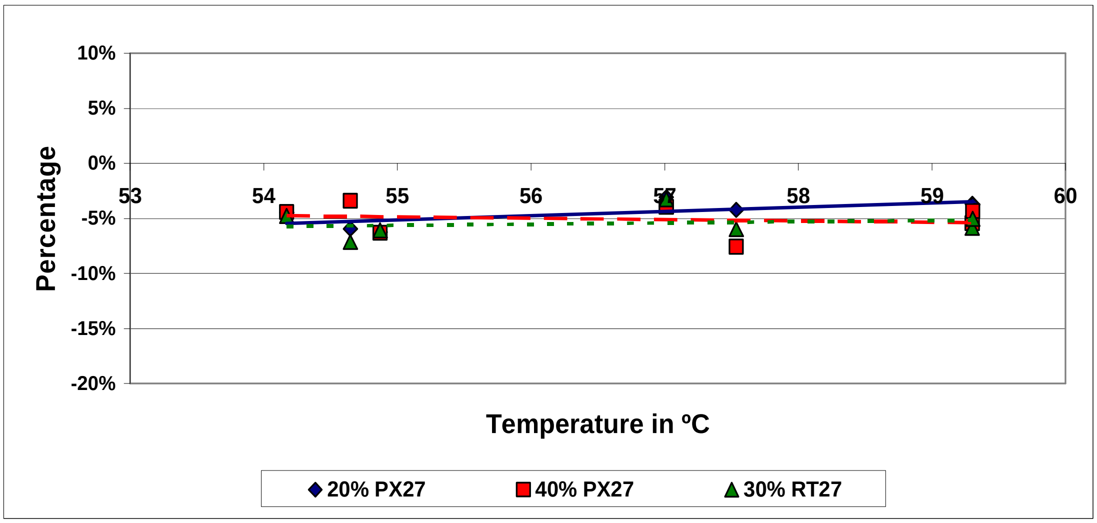

Figure 35. Comparison of Averaged Total Daily Heat Flow Reduction for the PX27 and RT27 Tests

To determine what the length of the heating period would have on the performance of the SP27 and the RT27 at these concentrations, tests were performed at a 7-hour and 6-hour heating duration. Shorter heating periods might represent walls with a shorter exposure to the sun’s heat, such as east facing walls. Results of these tests are presented in Table 18 for the 7-hour heating period and Table 19 for the 6-hour heating period respectively.

Table 18. Averaged Peak Heat Flux and Total Daily Heat Flow Reductions of PX27 and RT27 for 7-Hour Heating Period

Peak Heat Flux and Percent Reduction

	Max Temp *		Control		20% PX27			40% PX27			30% RT27		
Test #	℃	℉	W/m^2	$Btu/hr{\cdot}ft^2$	W/m^2	$Btu/hr{\cdot}ft^2$	Reduction	W/m^2	$Btu/hr{\cdot}ft^2$	Reduction	W/m^2	$Btu/hr{\cdot}ft^2$	Reduction
1	54.7	130.47	15.10	4.79	16.03	5.08	-6.2%	14.04	4.45	7.0%	14.82	4.70	1.8%
2	54.2	129.64	14.73	4.67	14.80	4.69	-0.5%	13.62	4.32	7.6%	14.28	4.53	3.1%
3	56.2	133.19	15.80	5.01	15.91	5.05	-0.7%	14.11	4.48	10.7%	15.27	4.84	3.3%
	Average		**15.21**	**4.82**	**15.58**	**4.94**	**-2.5%**	**13.92**	**4.42**	**8.4%**	**14.79**	**4.69**	**2.7%**

Total Heat Flow and Percent Reduction

	Max Temp *		Control		20% PX27			40% PX27			30% RT27		
Test #	℃	℉	$W/m^2{\cdot}day$	$Btu/day{\cdot}ft^2$	$W/m^2{\cdot}day$	$Btu/day{\cdot}ft^2$	Reduction	$W/m^2{\cdot}day$	$Btu/day{\cdot}ft^2$	Reduction	$W/m^2{\cdot}day$	$Btu/day{\cdot}ft^2$	Reduction
1	50.5	122.83	105.68	33.52	123.29	39.11	-16.7%	129.76	41.16	-22.8%	123.71	39.24	-17.1%
2	50.8	123.50	106.36	33.73	120.50	38.22	-13.3%	128.28	40.69	-20.6%	123.24	39.09	-15.9%
3	55.9	132.59	138.83	44.04	143.94	45.66	-3.7%	136.10	43.17	2.0%	140.96	44.71	-1.5%
	Average		**116.96**	**37.10**	**129.25**	**40.99**	**-11.2%**	**131.38**	**41.67**	**-13.8%**	**129.30**	**41.01**	**-11.5%**

* Max Temp is the maximum wall surface temperature in the interior of the simulator. The interior of the simulator represented the exterior of a typical building.

Table 19. Averaged Peak Heat Flux and Total Daily Heat Flow Reductions of PX27 and RT27 for 6-Hour Heating Period

Peak Heat Flux and Percent Reduction

	Max Temp *		Control		20% PX27			40% PX27			30% RT27		
Test #	℃	℉	W/m^2	$Btu/hr \cdot ft^2$	W/m^2	$Btu/hr \cdot ft^2$	Reduction	W/m^2	$Btu/hr \cdot ft^2$	Reduction	W/m^2	$Btu/hr \cdot ft^2$	Reduction
1	50.5	122.83	12.85	4.08	13.21	4.19	-2.8%	10.79	3.42	16.0%	12.05	3.82	6.2%
2	50.8	123.50	13.79	4.37	13.94	4.42	-1.1%	11.25	3.57	18.4%	12.50	3.96	9.4%
3	55.9	132.59	14.51	4.60	14.95	4.74	-3.0%	12.40	3.93	14.6%	13.99	4.44	3.6%
	Average		**13.72**	**4.35**	**14.03**	**4.45**	**-2.3%**	**11.48**	**3.64**	**16.3%**	**12.85**	**4.08**	**6.4%**

Total Heat Flow and Percent Reduction

	Max Temp *		Control		20% PX27			40% PX27			30% RT27		
Test #	℃	℉	$W/m^2 \cdot day$	$Btu/day \cdot ft^2$	$W/m^2 \cdot day$	$Btu/day \cdot ft^2$	Reduction	$W/m^2 \cdot day$	$Btu/day \cdot ft^2$	Reduction	$W/m^2 \cdot day$	$Btu/day \cdot ft^2$	Reduction
1	50.5	122.83	128.45	40.74	133.39	42.31	-3.9%	134.24	42.58	-4.5%	135.40	42.95	-5.4%
2	50.8	123.50	118.39	37.55	124.63	39.53	-5.3%	120.15	38.11	-1.5%	124.13	39.37	-4.8%
3	55.9	132.59	141.83	44.99	149.24	47.34	-5.2%	148.03	46.95	-4.4%	151.44	48.03	-6.8%
	Average		**129.56**	**41.09**	**135.75**	**43.06**	**-4.8%**	**134.14**	**42.55**	**-3.5%**	**136.99**	**43.45**	**-5.7%**

* Max Temp is the maximum wall surface temperature in the interior of the simulator. The interior of the simulator represented the exterior of a typical building.

In both the 7-hour and 6-hour heating cycles, the 40% PX27 wall and the 30% RT27 wall had a reduction of peak heat flux and an increase in total daily heat flow. In both heating cycles, the 20% PX27 had an increase in peak heat flux and total daily heat flow. These results were similar to the tests performed with an 8-hour heating cycle.

To compare the performance in these walls, the peak heat flux reduction and the total daily heat flow for the three walls at each heating duration is tabulated in Table 20. These results show that the performance of the walls worsened with the 7-hour heating cycle, but seemed to recover with the 6-hour heating cycle, more so with the 40% PX27 and 30% RT27. In fact, based on these tests, the later two walls perform better with the 6-hour heating cycle than the 8-hour heating cycle.

Table 20. Averaged Peak Heat Flux and Total Daily Heat Flow Reduction of PX27 and RT27 for 8-, 7-, and 6-Hour Heating Period

Average Peak Heat Flux Reduction	20% PX27	40% PX27	30% RT27
8-hour heating period	-2.7%	9.3%	4.3%
7-hour heating period	-2.9%	7.4%	2.0%
6-hour heating period	-2.3%	16.3%	6.4%

Average Total Heat Flow Reduction	20% PX27	40% PX27	30% RT27
8-hour heating period	-4.5%	-5.1%	-5.4%
7-hour heating period	-11.2%	-13.8%	-11.5%
6-hour heating period	-4.8%	-3.5%	-5.7%

Performance of PX27

To compare the performance of the three concentrations of PX27-enhanced cellulose insulation tested (10%, 20%, and 40%), the reduction in average peak heat flux and average total daily heat flow was tabulated in Table 21. These tests were with 8 hours of heating only. Each reduction calculated was the percentage difference of the peak heat flux and total daily heat flow of each test wall compared to that of the control wall.

Table 21. Comparison of the Reduction in Averaged Peak Heat Flux and Total Daily Heat Flow for PX27 Test Walls

	10% PX27	20% PX27	20% PX27 (retest)	40% PX27
Average Peak Heat Flux Reduction	-1.3%	-3.2%	-2.7%	9.3%
Average Total Heat Flow Reduction	-1.1%	-4.0%	-4.5%	-5.1%

As the results show, only the 40% PX27 concentration provided a peak heat flux reduction. Both the 10% and 20% concentrations of PX27 yielded an increase in both peak heat flux and total daily heat flow. All three concentrations yielded an increase in total daily heat flow. These results indicated that there may not have been a sufficient amount of the PCM material in the 10% and 20% concentrations to provide thermal storage benefit, but that at a higher concentration, the PX27 PCM showed a great potential for peak energy savings.

It should be noted that the 20% PX27 wall was tested twice, once with the 10% PX27 wall and again with the 40% PX27 wall. The results are shown for both 20%

PX27 tests to prove the repeatability of the tests. Both tests yielded similar results: approximately 3% reduction in peak heat flux and approximately 4.25% increase in total daily heat flow.

Performance of RT27

To compare the performance of all three concentrations of RT27-enhanced cellulose insulation (10%, 20%, and 30%), the reduction in average peak heat flux and average total daily heat flow was tabulated in Table 22 (also Figure 36). These tests were with 8 hours of heating only. Each reduction calculated was the percentage difference of the peak heat flux and total daily heat flow of each test wall compared to that of the control wall.

Table 22. Comparison of the Reduction in Averaged Peak Heat Flux and Total Daily Heat Flow for RT27 Test Walls

	10% RT27	**20% RT27**	**30% RT27**
Average Peak Heat Flux Reduction	5.7%	9.2%	4.3%
Average Total Heat Flow Reduction	0.6%	1.2%	-5.4%

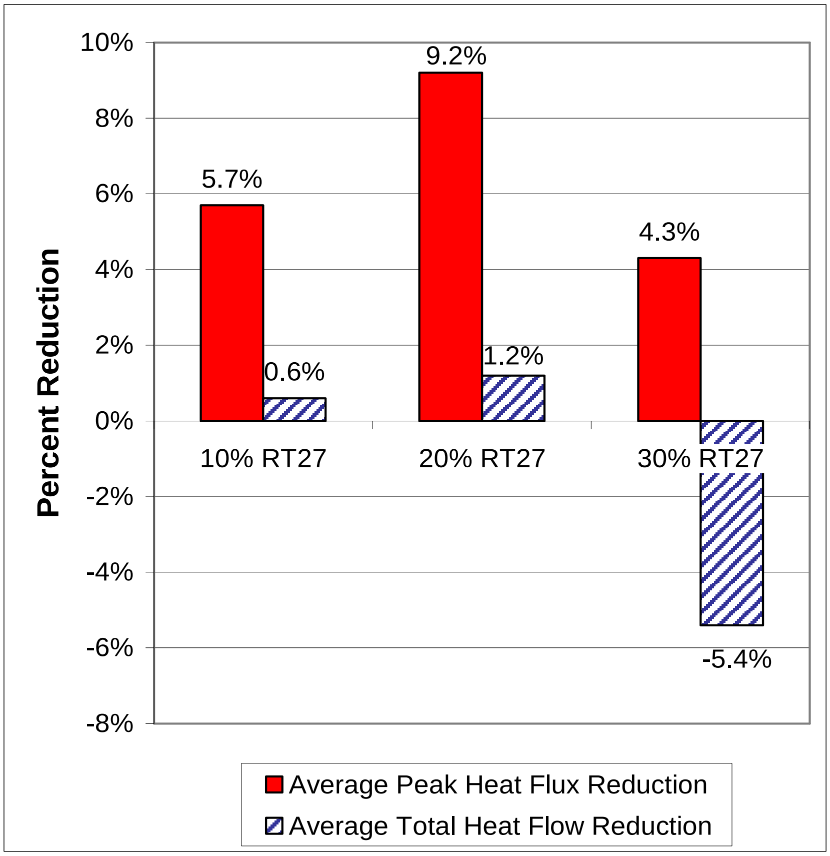

Figure 36. Comparison of Performance of RT27 PCM at 10%, 20%, and 30% Concentrations

As the results show, the 20% RT27 insulation provided nearly twice the percentage reduction of peak heat flux and twice the percentage reduction of total daily heat flow of the 10% RT27 insulation. Since there was twice as much PCM in the 20% RT27 insulation than the 10% RT27, it would appear that there may be a linear relationship between the amount of PCM added to the insulation and the energy savings. In other words, if twice the amount of PCM were added to the cellulose insulation, it would follow that twice the energy savings would have resulted. However, the results of the 30% RT27 test did not follow this pattern. At the 30%

concentration, there was an even lower reduction in peak heat flux than the 10% concentration and an increase in total daily heat flow. This drop in thermal performance might have been the result of incomplete melting of the larger amount of RT27 paraffin PCM. As previously stated, the total daily heat flow reductions in 10% and 20% RT27 walls may have been more pronounced if the simulator's interior would have been cooler than its exterior as may be the case in a building under full weather conditions. Similarly, the total daily heat flow increase from the 30% RT27 wall make have been lowered.

From these results, a PCM/cellulose mixture with a concentration of 20% for the RT27 PCM appeared to provide the maximum energy savings.

Observations

The melted PCMs (RT27, TH29, TH24, and SP25) adhered well to the cellulose material, and there was no indication of settling of the PCM in the cellulose insulation (i.e., no settling of PCM to the bottom of the insulation cavity) with the exception of the powdered paraffin PX27. There was little evidence of settling of the PCM/cellulose material within the wall. In a few cases, the material had dropped and left about 1.5 cm (0.6 in.) of airspace at the top of the cavity (Figure 37).

Figure 37. Interior View of Frame Wall Showing Little Evidence of Settling

The powdered PCM, PX27, mixed well with the cellulose material, but when the enhanced cellulose was moved, the powdered PCM immediately began to settle within the cellulose insulation. When the PX27 was being blown into the wall cavity via the insulation blower, the powdered material separated from the cellulose insulation and dropped to the bottom of the hopper cavity. Figure 38 shows the powdered PX27 settled out of the cellulose insulation. While the PX27 PCM settled out of the insulation during handling and insulation, there was no evidence that the PCM material settled (i.e. migrated downward) within the insulation in the wall cavity.

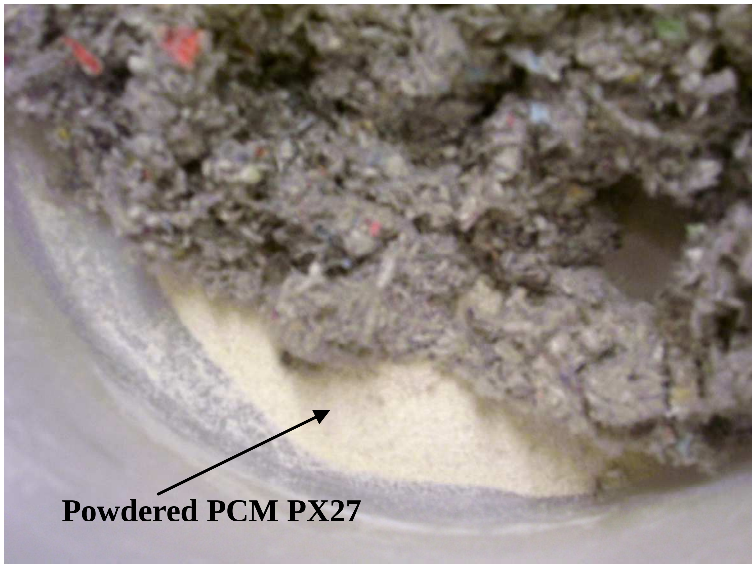

Figure 38. View of Settled Powdered PCM PX27 in Cellulose Insulation

In the walls that held the liquid/solid paraffin PCM RT27, there was evidence of discoloration on the wood surfaces and the wallboard backing particularly with the higher concentrations of paraffin (20%, 40%) as shown in Figures 39 and 40. There was no evidence of deterioration on these surfaces.

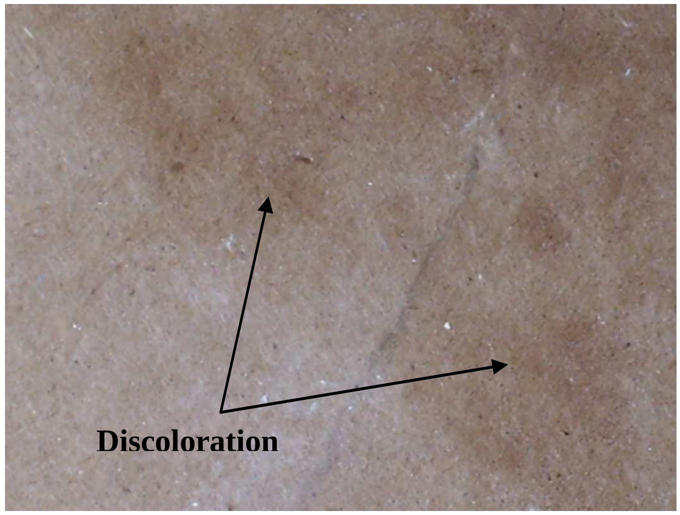

Figure 39. Discoloration on Wallboard Backing

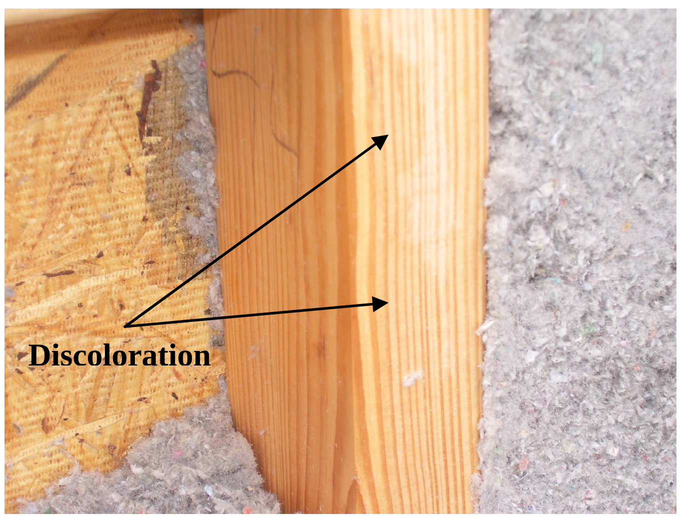

Figure 40. Discoloration on Stud

On the walls that held the hydrated salt PCMs, TH29 and TH24, there was evidence of corrosion on the exposed metal of the staples as shown in Figure 41. This was observed on the interior and the exterior of the wallboard.

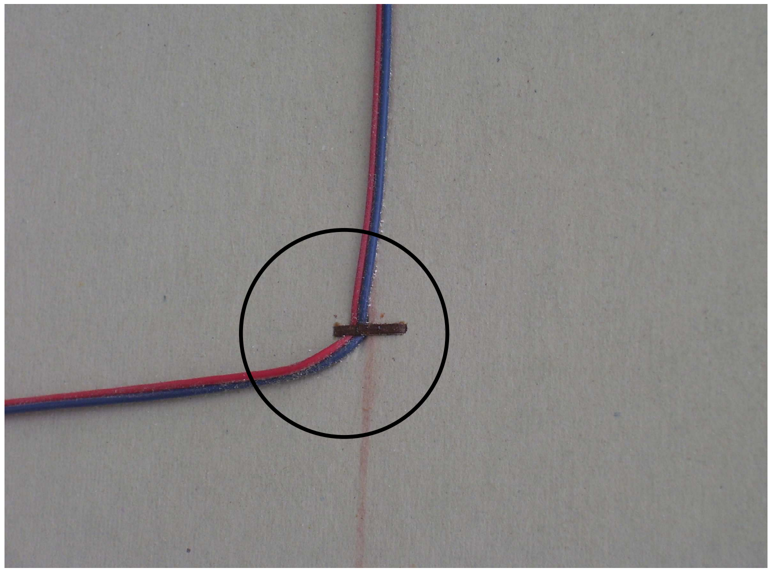

Figure 41. Corrosion on Staples of TH29 Hydrated Salt Wall

Flammability Test Results

To determine the flammability of the PCM-enhanced insulation, each PCM-enhanced insulation material was tested for critical radiant flux as required for conventional cellulose insulation under the Code of Federal Regulations (ASTM C-739). This test, also known as the flame spread test, requires that cellulose insulation have a critical radiant flux of no less than 0.120 watts/cm^2. Critical radiant flux is the radiant energy required for a flame to spread across the surface of the insulation material. A series of flame spread tests were performed with an electric radiant panel at a temperature of 140°F at Central Fiber Corporation. Results of the flammability test for each PCM-enhanced insulation material (in various PCM concentrations) are shown Table 23.

Table 23. Results of Flammability Tests

PCM	Result
10% RT27	combust; fail
20% RT27	combust; fail
10% TH29	0.160 W/cm^2; pass
20% TH29	0.220 W/cm^2; pass
10% TH24	0.160 W/cm^2; pass
20% TH24	0.179 W/cm^2; pass
10% SP25	>0.227 W/cm^2; pass
20% PX27	0.188 W/cm^2; pass*
40% PX27	combust; fail

*** Note:** Material continued to burn in charred area. NOT recommended.

As shown in Table 23, the liquid/solid paraffin PCM, RT27, failed the flammability test while the hydrated salt PCMs (TH24, TH29, and SP25) passed the test at all concentrations. The RT27 PCM failed because of the flammable property of paraffin. The powdered paraffin PCM, PX27, passed at the 20% concentration, however this substance could not be recommend as an additive because the material continued to burn in the charred area [28]. The test at the 40% concentration failed proving that the PX27-enhanced insulation was flammable depending on the concentration. It should be noted that the 30% RT27 PCM cellulose material was not tested because the RT27-enhance insulation at the lower concentrations failed the flammability test. Increasing the concentration of RT27 in the cellulose insulation would increase the flammability of the mixture and the material would certainly have failed the flammability test. For the RT27-enhanced cellulose insulation to pass the flame spread test, the flame retardant additives would have to be reformulated.

CHAPTER VI

ANALYSES

Equivalent Thermal Resistance

Because the RT27 PCM insulation at the 10% and 20% concentrations performed better than the other insulation materials in both peak heat flux reduction and total daily heat flow reduction, these mixtures were chosen for further analysis. The thermal resistance, or R-value, of insulation material is the measure of the amount of heat that flows through a particular section of wall at a certain temperature difference across the wall under steady state conditions. Specifically, R-value is calculated as the inverse of the heat flux through the wall multiplied by the temperature difference across the wall. Thermal performance of a particular insulation material may be gauged by its R-value. The higher the R-value, the higher the material's resistance to heat flow. In a typical day, a wall undergoes a cycle of heating and cooling and is constantly in a state of change. Equivalent thermal resistance is a measure of the apparent R-value at any given time during heating or cooling of the wall. Equivalent resistance could potentially be a good measurement of thermal performance for the PCM material as the thermal storage benefit of the PCM is manifested only in the phase change, during heating or cooling, and not under steady state conditions.

To evaluate the thermal performance of the RT27-enhanced insulation in the 10% and 20% concentrations, the equivalent thermal resistance of a representative test was determined and plotted in terms of the temperature difference across the wall (Figure 42). As seen in the curves shown in Figure 42, the equivalent thermal resistance, in both the test walls and the control wall, increased as the temperature difference across the wall increased. In other words, as the wall was heated the equivalent thermal resistance increased, more significantly in the PCM-enhanced walls when compared to the control wall. As the wall reached its maximum heating temperature, the RT27 walls reached a higher peak equivalent thermal resistance, 5.0 °C·m^2/W (28.6 °F·hr·ft^2/Btu) for the 10% RT27 wall and 6.4 °C·m^2/W (36.2 °F·hr·ft^2/Btu) for the 20% RT27 wall. These were significant increases of 25% higher for the 10% RT27 wall and 60% for the 20% RT27 wall compared to the peak equivalent thermal resistance of the control wall of 4.0 °C·m^2/W (22.0 °F·hr·ft^2/Btu).

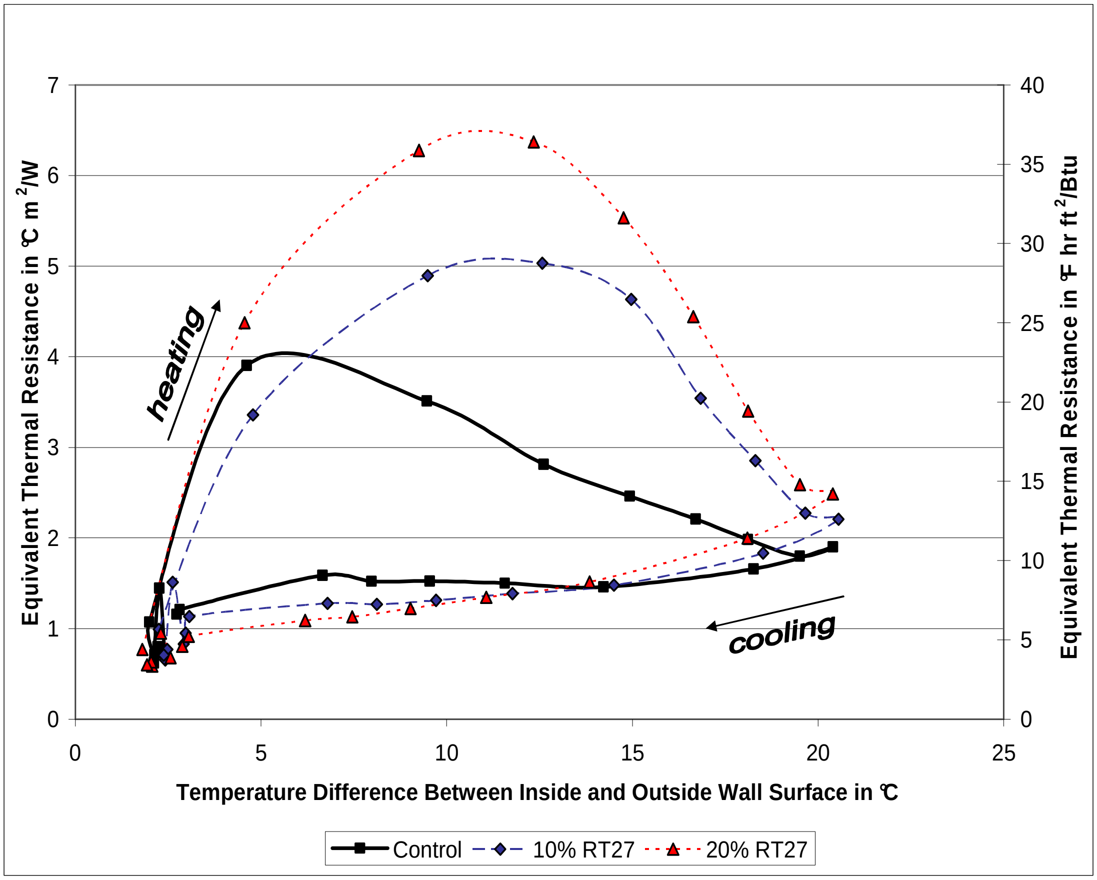

Figure 42. Equivalent Thermal Resistance for 10% RT27 and 20% RT27 Walls
Compared to the Control Wall

The increase in equivalent thermal resistance for the RT27-enhanced walls compared to the control wall showed that the RT27 material increased the walls thermal resistance during the heating process as it absorbed heat.

Potential Seasonal Energy Savings

To determine the potential energy savings from the 10% and 20% RT27 PCM walls, the total daily heat flow reduction for each wall was calculated as the difference in total daily heat flow between the control wall and the test walls. The averaged total daily heat flow reduction is tabulated in Table 24.

Table 24. Total Daily Heat Flow Reduction for 10% and 20% RT27 Walls

Control		10% RT27			20% RT27		
W/m^2·day	Btu/day·ft^2	Reduction	W/m^2·day	Btu/day·ft^2	Reduction	W/m^2·day	Btu/day·ft^2
158.12	50.15	0.6%	157.13	49.84	1.2%	156.27	49.57

As discussed previously, the total daily heat flow reductions from the 10% and 20% RT27 walls were smaller than what may have been measured under full weather conditions. Therefore, these reductions provided a conservative estimate of the potential energy savings. To estimate the potential seasonal energy savings in a summer season, the averaged total daily heat flow reduction was multiplied by the surface area normal to the insulated cavity and by the total number of days in the three months in summer or 90 days. The insulated cavity was 81.3 cm x 111.8 cm (32 in. x 44 in.) or 0.91 m^2 (1408 in^2). The energy savings potential in the test walls for one cooling season is shown in Table 25.

Table 25. Seasonal Energy Savings for 10% and 20% RT27 Walls

10% RT27		20% RT27	
kWh	Btu	kWh	Btu
0.08	275	0.15	515

As a conservative estimate, during the summer season, it may be possible to achieve up to 0.15 kWh (515 Btu) in energy savings for only a small wall of less than a square meter in size. For a single story 111.5 m^2 (1200 ft^2) home with 2.4 m (8 ft) walls and a 48.8 m (160 ft) perimeter, the area of the walls would be roughly 2.4 m x 48.8 m (8 ft x 160 ft) or 119 m^2 (1280 ft^2). Calculating the potential energy saving in this home by taking a ratio of wall areas multiplied by the test energy savings yielded a savings of 19.8 kWh (67,400 Btu). This was a simplified model of the summer cooling season since the solar energy changes in intensity over the summer months, but this method gave a rough estimate of the potential savings using this PCM material.

Embodied Energy

The goal of the incorporation of phase change materials was to save energy by means of thermal storage in the walls. In order to evaluate the overall energy savings of incorporating PCMs in walls, the energy used to manufacture, transport, and incorporate the PCM in to the wall system should be included in an energy savings evaluation. In other words, even though the use of PCMs have a significant energy savings, the use of the materials also has an energy cost. This added energy used to make the PCM-enhanced wall is termed embodied energy. By comparing the potential annual energy savings to the total embodied energy, a simple energy payback can be calculated. This simple energy payback is the number of years it would take for the total energy saved to surpass the embodied energy.

In calculating the embodied energy in the RT27 PCM, factors contributing to the energy used to make the RT27 walls were identified. These factors included the manufacturing of the RT27 PCM, the construction of the PCM wall system, and shipping of the PCM and the PCM-enhanced insulation. An energy usage per unit weight was determined for each of these contributing factors. The total energy per kilogram (lb.) multiplied by the total weight of the PCM used in the walls, gives the overall embodied energy in the PCM material.

The embodied energy in the manufacturing of the RT27 PCM material was 0.7 kWh/kg (1085.7 Btu/lb) [27]. This includes all the energy used to manufacture and package only the PCM product. The embodied energy of the cellulose and other building materials was not included in the calculation because these factors were the same for the control wall and for the PCM-enhanced wall. Only the difference of adding the PCM was taken into account in this analysis.

The embodied energy due to the construction of the PCM-enhanced wall was composed of two factors: incorporating the PCM into the cellulose insulation and installing the additional PCM-enhanced insulation into the wall. Only the energy from incorporating the PCM into the insulation and installing the additional PCM-enhanced insulation in to the wall was included in the calculation. In other words, the energy consumed to make the cellulose and build the basic wall was the same for both the control wall and the PCM-enhanced wall. In this research, the PCM was incorporated by hand into the cellulose insulation, but in reality, the PCM would be incorporated during the manufacturing of the cellulose insulation. During the insulation making process, the cellulose newsprint is agitated and mixed with additives (e.g. borax for fire retardation), at which time the liquid PCM would be sprayed on to the cellulose material. To incorporate the PCM into the cellulose insulation, a heating element and pump would be added to this step of the process [28]. The heating element would keep the paraffin PCM in a liquid state above the melting temperature and the pump would allow distribution of the PCM on to the cellulose material. For example, Central Fiber Corporation makes 4,086 kilograms per hour (9,000 lb/hr) of cellulose material. At a concentration of 20%, 2.2 kg (2.4 lb) of paraffin PCM RT27 would be added to the cellulose at a rate of 0.045 kiloliter per minute (12 gal/min). As a simple estimate of the energy used to incorporate the PCM during the manufacturing of the cellulose insulation, the heating element was assumed to be 1 kW (3,412 Btu) and the pump was assumed to be 0.75 kW (1 hp or 2,545 Btu/hr) pump [29]. Assuming the same production rate of 4,086 kg/hr (9,000 lb/hr), the energy used was 0.0004 kWh/kg (0.66 Btu/lb) for both the heating element and the pump. In the installation of the PCM-enhanced insulation into the wall, additional time was required to blow the cellulose in to the wall cavity with the added weight of the PCM at nearly the same volume. Estimating that the blower filled the wall cavity at a rate of 1.14 kg/min (2.5 lb/min) or 68 kg/hr (150 lb/hr) with a power rating of 0.56 kW (¾ hp or 1,909 Btu/hr), the energy used was 0.0082 kWh/kg (0.21 Btu/lb). In total, the energy used to make the PCM-enhanced wall was 0.0086 kWh/kg (0.87 Btu/lb). The energy used in the making of the PCM-enhanced wall is summarized in Table 26.

Table 26. Electricity Used in Construction of PCM/Cellulose Wall System

	Power rating		Production Rate		Energy per unit weight	
Equipment	**kW**	**Btu/hr**	**kg/hr**	**lb/hr**	**kWh/kg**	**Btu/lb**
Heating element	1.00	3,412	4,086	9,000	0.0002	0.38
Pump	0.75	2,545	4,086	9,000	0.0002	0.28
Blower	0.56	1,909	68	150	0.0082	0.21
Total					**0.0086**	**0.87**

The transport of the PCM material from the manufacturer to the cellulose producer and then to the consumer uses energy that must be included in the embodied energy analysis. The average energy intensity for inter-city freight movement by truck was 2.43 kJ/kg-km or 0.674 Wh/kg-km (3,357 Btu per ton-mile) [30]. Assuming that the PCM manufacturer is within 482.8 kilometers (300 mi) of the cellulose manufacturer and that the consumer is also within 482.8 kilometers (300 mi) of the cellulose manufacturer, a distance of 965.6 kilometers (600 mi) was used to calculate energy consumed during transportation by truck. The total energy per unit weight attributable to transportation was 0.65 kWh/kg (1,007 Btu/lb).

For the walls used in this research, 1.1 kg (2.4 lb) of RT27 was added to the 10% RT27 wall and 2.2 kg (4.8 lb) of RT27 was added to the 20% RT27 wall. Only the weight of the PCM was included in this calculation because the weight of the insulation and other building materials would be the same for both the control wall and the PCM-enhanced wall. By multiplying these weights by the total energy per unit weight, the embodied energy of the wall were calculated as approximately 1.5 kWh (5,025 Btu) for the 10% RT27 wall and 3.0 kWh (10,049 Btu) for the 20% RT27 wall. The embodied energy calculation is summarized in Table 27.

Table 27. Embodied Energy by Process for 10% and 20% RT27 PCM

	Energy per unit weight		Embodied Energy 10% RT27				Embodied Energy 20% RT27			
Process	**kWh/kg**	**(Btu/lb)**	**kg**	**lb**	**kWh**	**Btu**	**kg**	**lb**	**kWh**	**Btu**
Manufacturing of PCM	0.70	1085.64	1.1	2.4	0.77	2,606	2.2	4.8	1.54	5,211
Construction of Wall	0.0086	0.87	1.1	2.4	0.0095	2	2.2	4.8	0.0190	4
Transportation	0.65	1007.10	1.1	2.4	0.71	2,417	2.2	4.8	1.43	4,834
Total Energy Used					**1.49**	**5,025**			**2.99**	**10,049**

To compare the embodied energy to the potential energy savings in the tests walls, a ratio of embodied energy to potential energy savings was calculated (Table 28). The simple energy payback for the 10% RT27 wall was approximately 18.5 cooling seasons and the simple energy payback for the 20% RT27 wall was 19.5 cooling seasons. In other words, in terms of energy, the use of RT27 PCM in walls at these concentrations may save as much energy as was used to create the PCM-enhanced walls in a rather long period of time. If the use of PCMs during the heating season (in the winter months) was taken into account, this simple payback may be reduced. That is, as the PCM provided energy savings in the wintertime by reducing the amount of heat that is lost from the heated interior of the building, the simple payback period may be less than estimated in cooling seasons.

Table 28. Simple energy payback for 10% and 20% RT27 PCM

	10% RT27 Wall		**20% RT27 Wall**	
	kWh	**Btu**	**kWh**	**Btu**
Potential Energy Savings	0.08	275	0.15	515
Embodied Energy	1.49	5,025	2.99	10,049
Simple Energy Payback	**18.5 years**		**19.5 years**	

The values in Table 28 of 18.5 years and 19.5 years are high because the low percent reductions provided by the simulator were used to estimate the energy savings. In general, while the use of PCMs may produce an immediate energy savings to the consumer, the energy "cost" may be much larger than the annual potential energy savings.

CHAPTER VII

CONCLUSIONS AND RECOMMENDATIONS

It can be concluded that the liquid/solid paraffin PCM RT27 performed better than the other PCMs tested. Incorporating the paraffin PCM RT27 into wall cavities, in both 10% and 20% concentrations, reduced the peak heat flux across a wall and provided a time shift of the peak heat flux in the paraffin-enhanced walls as compared to the control wall. On average, the 10% RT27 wall reduced the peak heat flux by 5.7% and the 20% RT27 wall reduced the peak heat flux by 9.2%. These paraffin-enhanced walls also provided a reduction in total heat flow, albeit only a slight reduction of 0.6% for the 10% RT27 wall and 1.2% for the 20% RT27 wall. These reductions in heat transferred through the walls were conservative estimates, however would result in lowered energy cost associated with conditioning the interior of buildings. Conversely, at the 30% concentration, the thermal performance of the RT27 decreased. The 30% RT27 insulation decreased the peak heat flux by only 4.3% and increased the total daily heat flow by 5.4%. As discussed previously, the total daily heat flow in this test wall may have been lower than the control wall had the test been performed under full weather conditions and the percent reduction would have been higher. Overall, the RT27 PCM mixed well with the cellulose insulation with no evidence of settling or separation of the materials. There was some discoloration to the interior structure of the insulation cavity caused by the paraffin PCM, but no damage to the wood or wallboard. The major disadvantage of incorporating RT27 in walls is its flammability. The RT27 failed flammability tests performed at any concentration. In all, RT27 PCM at certain concentrations may be a suitable medium for thermal storage in the walls of buildings provided the cellulose mixture is reformulated to address the flammability issue.

In one particular test, the equivalent thermal resistance of both the 10% RT27 and 20% RT27 was found to be 25% and 60% higher at its peak, thus increasing the insulations ability to resist heat that may travel through the wall. The potential seasonal energy savings were conservatively estimated to be up to 0.08 kWh (275 Btu) for the 10% RT27 wall and 0.15 kWh (515 Btu) for the 20% wall. This energy savings may be much larger and may translate into a noticeable financial savings for the consumer when applied to a full-scale residential structure. The use of PCM may also decrease the peak heat flux through the wall, and thus the peak demand to the cooling system, and may result in smaller air conditioning systems. The embodied energy of the RT27-enhanced walls was estimated to be 1.5 kWh (5,025 Btu) for the 10% RT27 wall and 3.0 kWh (10,049 Btu) for the 20% RT27 wall. By comparing the potential energy savings to the embodied energy of the RT27 walls, the incorporation of the RT27 PCM into the walls may provide a simple energy payback of 18.5 cooling seasons for the 10% concentration and 19.5 cooling seasons for the 20% concentration. In other words, the energy cost of the RT27 PCM is “paid off” over a rather long time period. Since the total daily heat flow may be reduced under full weather conditions and since there would be an energy savings associated with the use of PCMs in the wintertime, this simple payback period may be less than estimated in cooling seasons. Overall, with the long-term effectiveness of the RT27-enhanced insulation still unknown, the feasibility of the use of the RT27 PCM cannot be determined over such a long period of time.

The powdered PCM PX27 performed well to reduce the peak heat flux through the wall at an average of 9.3% for the 40% concentration, but did not reduce the total daily heat flow likely due to the limitations of the simulator. With a shorter heating period of 6 hours, the PX27 insulation’s performance increased to an average of 16.3% for the 40% concentrations. At lower concentrations, the PX27 did not reduce the peak heat flux, nor reduce the total daily heat flow. This was certainly due to the fact that the powdered material settled out of the insulation mixture. Also, the higher concentration of PX27 failed flammability tests. Overall, the PX27 shows potential as a thermal storage medium at higher concentrations, but again additives would need to be incorporated to reduce its flammability.

The hydrated salt PCMs TH29 and TH24, as well as the eutectic PCM SP25, did not decrease the peak heat flux across the wall at any concentrations in any tests performed, and in turn increased the heat transferred through the wall significantly, likely because of the hydroscopic properties of the hydrated salt combined with its higher conductivity. For this reason, it can be concluded that hydrated salt-based PCMs do not provide any benefit as a method of thermal storage unless they are encapsulated in some fashion.

It is recommended that the paraffin-based PCM-enhanced insulation (RT27 and PX27) be developed during production incorporating fire-retardant additives to reduce their flammability. For the PX27 PCM, it is recommended that a smaller diameter powder be incorporated into the cellulose material so that the material might stay in mixture and not settle to the bottom of the insulation. Long-term testing should be performed to determine the effectiveness of the RT27 and PX27 materials after long exposure to air and the heating/cooling cycle. Tests with different heating lengths should be performed to model walls with different exposure to the sun's radiation (i.e. north/south/east/west exposure). Likewise, since these test results indicated that the paraffin-based PCMs performs better at lower heating temperatures, more tests at these lower temperatures may help determine in which types of climates (cooler/milder versus warmer) the PCMs would be most effective.

The hydrated-salt based PCMs (TH29, TH29-F127, TH24, and SP25) should only be tested if these PCMs are macro-encapsulated. Unique methods of encapsulation in wall should be investigated and developed.

It is also recommended that some type of refrigeration or ventilation be added to the interior of the simulator during the cool down period so that the interior could cool to a temperature below the temperature of the conditioned space. This would allow the simulator to more closely model a building wall under full weather conditions.

REFERENCES

[1] Department of Energy Buildings Energy Data Book, 2007, <http://www.btscoredatabook.net>

[2] United States Consumer Products Safety Commission, Code of Federal Regulations, Title 16, Part 1209, Safety Standards for Cellulose Insulation, 2008. <http://ecfr.gpoaccess.gov/cgi/t/text/text-idx?sid=28d187081ad77fb71884ea1e89ff568b&c=ecfr&tpl=/ecfrbrowse/Title16/16cfrv2_02.tpl>.

[3] Department of Energy Insulation Fact Sheet, 2008, <http://www.ornl.gov/sci/roofs+walls/insulation/ins_06.html>

[4] D.W. Hawes, D. Feldman, D. Banu, Latent heat storage in building materials, Energy and Buildings, 1993; v. 20, 77–86

[5] V.V. Tyagi, D. Buddhi, PCM thermal storage in buildings: A state of art, Renewable & Sustainable Energy Reviews, 2007, v. 11, n. 6, 1146–1166

[6] M. Telkes, Storage of solar heating/cooling, ASHRAE Transactions, 1974, v. 80, n. Part 2, 382–392

[7] D. Feldman, D. Banu, D.W. Hawes, Development and application of organic phase change mixtures in thermal storage gypsum wallboard, Solar Energy Materials and Solar Cells, 1995, v. 36, 147–157

[8] S. Scalat, D. Banu, D. Hawes, J. Paris, F. Haghighat, D. Feldman, Full scale thermal testing of latent heat storage in wallboard, Solar Energy Materials and Solar Cells, 1996, v. 44, 49–61.

[9] M.N.A. Hawlader, M.S. Uddin, Mya Mya Khin, Microencapsulated PCM thermal-energy storage system, Applied Energy, 2003. v. 74, 195–202.

[10] M. Zhang, M.A. Medina, and J. B. King, Development of a thermally enhanced frame wall with phase-change materials for on-peak air conditioning demand reduction and energy savings in residential buildings, International Journal of Energy Research, 2005, v. 29, 795–809.

[11] I.O. Salyer, A.K. Sircar, Review of phase change materials research for thermal energy storage in heating and cooling applications at the University of Dayton from 1982 to 1996, International Journal of Global Energy Issues, v. 9, n. 3, 1997, p 183–198

[12] J.B. King, Preliminary Evaluation of the Thermal Performance of Phase Change Material - Structural Insulated Panels (PCM-SIPs). Thesis. Univ. of Kansas, 2004.

[13] D. Zhu, A Comparative Heat Transfer Examination of Structural Insulated Panels (SIPs) with and without Phase Change Materials (PCMs) Using a Dynamic Wall Simulator. Thesis. Univ. of Kansas, 2005.

[14] Y.P. Zhang, K.P Lin, R.Yang, H.F. Di, Y. Jiang, Preparation, thermal performance and application of shape-stabilized PCM in energy efficient buildings, Energy and Buildings, 2006, v 38, n 10, p 1262-1269

[15] Y.P. Zhang, X. Xu, H. Di, K. Lin, R. Yang, Experimental study on the thermal performance of the shape-stabilized phase change material floor used in passive solar buildings, Journal of Solar Energy Engineering, Transactions of the ASME, 2006, v 128, n 2, p 255-257

[16] J. Kosny, D. Yarbrough, W. Miller, T. Petrie, P. Childs, A. Syed, and D. Leuthold, Thermal performance of PCM-enhanced building envelope systems, Thermal Performance of the Exterior Envelopes of Buildings X, proceedings of ASHRAE THERM X, Clearwater, FL, Dec. 2007.

[17] J. Kosny, Oakridge National Laboratories, private communications, 2004

[18] TH29 Phase Change Material (PCM) Data Sheet, European Thermodynamics, 2002, <http://www.europeanthermodynamics.com/TEAP%20PCM/TH29%20Data%20Sheet.pdf>.

[19] I. Šateikis, Research results of heat storage for air heating using the capsules of calcium chloride hexahydrate, XL Scientific Conference, 22 Nov. 2002, Estonian Agricultural University

[20] Product Information, TEAP Energy, 2007, <http://www.teappcm.com/products/general.htm>

[21] Rubitherm RT Product Information, Rubitherm Technologies, 2006, <http://www.rubitherm.com/english/download/latent_heat_paraffins_rt27_ds.pdf>.

[22] Rubitherm SP Product Information, Rubitherm Technologies, 2006, <http://www.rubitherm.com/english/download/latent_heat_blend_sp25_ds.pdf>

[23] Rubitherm PX Product Information, Rubitherm Technologies, 2006, <http://www.rubitherm.com/english/download/latent_heat_powder_px27_ds.pdf>

[24] Central Fiber Corporation, <http://www.centralfiber.com>

[25] Force/1 Insulation Blower Information, Intec Corporation, <http://www.inteccorp.com/Force1.htm>

[26] M. Zhang, Performance Evaluation of a Phase Change Frame Wall. Thesis. Univ. of Kansas, 2004

[27] K. Fieback, Rubitherm Technologies, private correspondence, 2008

[28] D. Trieu, Central Fiber Corporation, private correspondence, 2008

[29] Iwaki America, pump information, <http://www.iwakiamerica.com/products/wmd.htm>

[30] State Actions: Washington, U.S. Environmental Protection Agency, 2008, <http://yosemite.epa.gov/gw/StatePolicyActions.nsf/uniqueKeyLookup/MSTY5Q4MSV?OpenDocument>